Toxicokinetics, dose-response and risk assessment of nanomaterials: methodology, challenges, and future perspectives

Qiran Chen[1,2], **Jim E. Riviere**[3,4], **Zhoumeng Lin**[1,2]

[1]Department of Environmental and Global Health, College of Public Health and Health Professions, University of Florida, Gainesville, Florida, USA.

[2]Center for Environmental and Human Toxicology, University of Florida, Gainesville, Florida, USA.

[3]1Data Consortium, Kansas State University, Olathe, Kansas, USA.

[4]Center for Chemical Toxicology Research and Pharmacokinetics, Department of Population Health and Pathobiology, College of Veterinary Medicine, North Carolina State University, Raleigh, North Carolina, USA.

Abstract

The rapid growth of nanomaterial applications has raised safety concerns for human health. A number of studies have been conducted to assess the toxicokinetics, toxicology, dose-response, and risk assessment of different nanomaterials using *in vitro* and *in vivo* animal and human models. However, current studies cannot meet the demand for efficient assessment of toxicokinetics, dose-response relationships nor the toxicological risk arising from the rapidly increasing number of newly synthesized nanomaterials. In this article, we review the methods for conducting toxicokinetics, hazard identification, dose-response, exposure and risk assessment studies of nanomaterials, identify the knowledge gaps, and discuss the challenges remaining. We provide the rationale behind the appropriate design of nanomaterial plasma toxicokinetic and tissue distribution studies, including caveats on the interpretation and correlation of *in vitro* and *in vivo* toxicology studies. The potential of using physiologically based pharmacokinetic (PBPK) models to extrapolate toxicokinetic and toxicity findings from *in vitro* to *in vivo* and from animals to humans is discussed, and the knowledge gaps of PBPK modeling for nanomaterials are identified. While challenges still exist, there has been progress in the toxicokinetics, hazard identification, and risk assessment of nanomaterials in the past two decades. Recent advancements in the field are highlighted with relevant examples. We also share latest guidelines as well as our perspectives on future studies needed to characterize the toxicokinetics, toxicity, and dose-response relationship in support of nanomaterial risk assessment.

Graphical Abstract

Correspondence: Zhoumeng Lin, Department of Environmental and Global Health, College of Public Health and Health Professions, University of Florida, 1225 Center Dr., Gainesville, Florida, 32610, USA. linzhoumeng@ufl.edu.
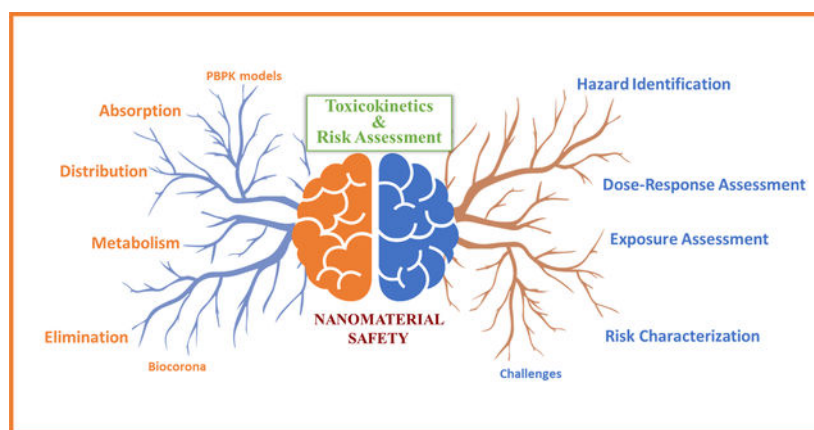
This article summarizes the methods for toxicokinetics, hazard identification, dose-response, exposure and risk assessment studies of nanomaterials, identifies the knowledge gaps, discusses the main challenges, and shares the latest guidelines and our perspectives on future studies.

Keywords

Nanomaterials; nanoparticles; toxicokinetics; risk assessment; dose-response assessment

1. INTRODUCTION

In the past two decades, nanotechnology has produced a large variety of nanomaterials (NMs) or nanoparticles (NPs) with different physicochemical properties, with a number of these products being widely used in consumer and industrial applications. This rapid growth of NM applications raises concerns over the safety of NMs on human health. The development, production, and application of NMs often incorporate pharmacokinetics/ toxicokinetics (PK/TK), toxicology and risk assessment studies using *in vitro* and *in vivo* animal models to understand and assess their impact on human health (Graham et al., 2017). However, current toxicokinetic, dose-response and risk assessment studies have not kept pace with the rapid increase in the number of newly synthesized NMs. This requires the development of higher level and more generalized computational modeling approaches to better quantitate these effects and thereby allow extrapolation to humans where such toxicity studies often cannot be directly conducted.

Our group previously reviewed the PK/TK properties and PK modeling studies of different NPs, including carbon nanotubes, fullerenes, quantum dots, gold (AuNPs), silver (AgNPs), iron oxide, titanium dioxide (TiO_2) and zinc oxide (ZnO) NPs (Z. Lin et al., 2015; Riviere, 2009; Riviere et al., 2013). More recently, several new PK/TK studies have been conducted (Table 1) and several reviews published (Arami et al., 2015; Badrigilan et al., 2020; Cheng et al., 2020; Hauser & Nowack, 2019), including a few on NM risk assessment (Kuempel et al., 2012; Oomen et al., 2018; Ramachandran, 2016). Existing reviews often focus on either specific PK/TK or risk assessment studies separately, making the linkage of TK properties to toxicity, dose-response relationships and risk assessment difficult. To address this scientific gap, the present review article will focus on the TK, toxicity dose-response

and risk assessment of NMs. We will review relevant methodologies, identify knowledge gaps, discuss challenges to their application and utilization, and share our perspectives on future studies to advance this field.

2. TOXICOKINETICS

PK or TK describes the rate at which a certain chemical or NM enters the body through different exposure routes and quantitates its distribution to different tissues, metabolism and excretion from the body. The term PK is typically used for drugs, whereas the term TK is often used for environmental chemicals or toxicants. Since this article discusses the toxicity and risk assessment of NMs, we will use the term TK. Many *in vivo* studies have been conducted to assess the TK of different NMs (Table 1). The commonly used experimental animals are rodents (mice and rats); although other larger mammals including rabbits, monkeys, and pigs have also been employed (Hauser & Nowack, 2019; Z. Lin et al., 2015).

A typical TK study includes two components: plasma TK and tissue biodistribution. The goal of a pure TK study is to characterize the plasma profile, determine common TK parameter values, evaluate tissue accumulation and depletion profiles, and ultimately identify the target tissue of NM accumulation. In brief, the study design consists of administering a certain dosage of NMs to a homogenous population of animals via different routes of exposure, such as intravenous or intraperitoneal injection, and oral administration. The animals are grouped based on different treatments and examination time points. Before and at predefined time points after dosing, plasma and/or tissue samples are collected to quantify the amount or concentration of the NMs. To characterize the plasma TK profile, there could be multiple experimental designs (Figure 1), including (1) a replicate blood sampling approach where each animal is sacrificed at a predefined time point and blood is collected at this single time point for each animal, (2) a staggered blood sampling approach where multiple blood samples are collected in a non-destructive manner for each subgroup of animals at different time points from either the same or a different anatomical sampling site between time points (the number of samples depends on the volume of the sample and the size of the animal), and (3) a serial or repeated blood sampling approach which non-destructively collects blood samples at all scheduled time points to derive the individual concentration-time profiles for all animals (Valic et al., 2020).

Depending on the blood sampling approach, using a serial or repeated blood sampling design allows the plasma TK profile to be characterized for each animal using either non-compartmental or traditional compartmental models to calculate the common TK parameters: the absorption rate constant (Ka), terminal elimination rate constant (Ke), half-life ($t_{1/2}$), maximum observed concentration (Cmax), time to reach the maximum observed concentration (Tmax), clearance (Cl), area under the concentration curve (AUC), and volume of distribution (Vd). The mean and standard deviation of each of these parameters are then calculated for each treatment group. Use of the replicate or staggered sampling design results in limited data points for each animal (also called sparse data) and do not cover the entire TK profile. In this case, other TK computational methods, including simple naïve pooled data methods, complex nonlinear mixed-effect modeling, and

Bayesian approaches should be used to determine the central tendency and variability of these TK parameters. It must be stressed that a limitation of many of these approaches which characterizes the vast majority of NM studies published, is the small number of samples collected in small rodent (especially mouse) studies. This often results in bias being introduced when characterizing TK parameters such as $t_{1/2}$ due to the small number and limited time points of the samples taken.

For tissue samples, the replicate sampling approach must be used unless biopsies are collected. Since each animal contributes only one data point at one time point at sacrifice, in order to characterize the tissue depletion profile, the mean concentration of all animals in a subgroup at a specific time point is calculated. This mean concentration-time profile is used to calculate relevant TK parameters, such a tissue half-life and terminal elimination rate constant. Again, the timing of sampling of the original experimental design in these limited studies often can bias the values obtained in the analysis.

2.1. Absorption

Unlike exposure by intravenous injection in which 100% of NMs enter the systemic circulation with no absorption phase, dosing by extravascular routes including oral ingestion, inhalation, and dermal contact, the rate and extent of absorption are different depending on multiple factors.

Bioavailability and absorption rate constant (Ka) are two commonly used TK parameters to describe the extent and rate of absorption, respectively. Bioavailability can be calculated as the ratio of the area-under-curve (AUC) of plasma concentrations of a NM between a given exposure route and intravenous injection. The absorption rate constant is usually used in TK studies to describe the rate of which NMs enter into the systemic system and can be calculated using the method of residuals. This method estimates the plasma drug concentration versus time plot as if absorption were instantaneous and then uses the difference between the actual and estimated concentrations to form a residual line to determine K_a (i.e., the negative slope of the residual line) (Spruill et al., 2014). The absorption rate constant directly impacts the maximum concentration (Cmax), which is a key parameter that reflects the rate of absorption. Depending on the type of NMs, absorption is usually low due to the biologically large size of NMs with absorption decreasing as the size increases (i.e., size-dependent). NMs typically include materials with at least one external dimension in the nanometer range (1–100 nm), but it could be larger in agglomeration state and could be larger than or close to cell membrane pore size limits depending on the type of organs (Bachler, von Goetz, et al., 2015). For example, the oral absorption efficiency of AuNPs ranges from 0.37% for small sizes (1.4–2.8 nm) to only 0.01% for a larger size (200 nm) (Schleh et al., 2012). While the oral bioavailability of NMs is generally very low, some organic NMs can be synthesized to encapsulate drugs that have poor solubility and low bioavailability, thereby improving the bioavailability of these normally poorly absorbed drugs. An example is astaxanthin which has poor solubility and low bioavailability. Its oral bioavailability can be improved 38-fold after encapsulation with poly (ethylene glycol)-graft-chitosan NPs (Zhu et al., 2022). Even though absorption of NMs is typically low following extravascular routes of administration, it is important to

note that NMs can interact with the portal of entry (e.g., respiratory tract, gastrointestinal tract, and skin), resulting in local effects (i.e., portal-of-entry effects) that may not be seen following a systemic intravenous administration. For example, pulmonary exposure to bolus doses of single-wall carbon nanotube (SWCNT) via pharyngeal aspiration caused granulomatous lesions associated with deposition of micrometer-sized agglomerates as well as rapid and progressive interstitial fibrosis related to migration of smaller sizes of SWCNT into the alveolar area (Oberdorster et al., 2015).

2.2. Distribution

NMs can distribute to almost all organs and tissues in the body after their initial absorption (Shi et al., 2013). The extent of distribution to an individual organ depends on the permeability of the capillary blood vessel, rate and extent of regional blood flow, and the membrane receptor affinity and abundance. For small molecules, the extent of distribution is described with the term "tissue:plasma partition coefficient", which represents the ratio of the concentrations of a chemical between tissue and plasma at thermodynamic equilibrium. However, this term is not applicable to NMs because NPs do not form solutions, but rather are colloidal dispersions, which are not thermodynamically stable (Praetorius et al., 2014). Therefore, the extent of tissue distribution of NMs are usually described using the term "distribution coefficient", which is the ratio of the concentrations of the NM between tissue and plasma at a certain time point or over a time period (Lin et al., 2008; Lin, Monteiro-Riviere, & Riviere, 2016; Utembe et al., 2020).

Biodistribution of NMs can be studied using either quantitative or semi-quantitative approaches. Intravenous dosing is the most commonly used administration route to study biodistribution of NMs. Following intravenous administration, a quantitative approach requires sacrificing groups of animals at different predetermined times, and then plasma and tissue samples collected to quantify the distribution profile of NMs to plasma and individual tissues. For example, Bailly et al. (2019) administrated 1 mg/kg of 21 nm AuNPs to three groups of six mice each, and then sacrificed the mice at different time points (1, 7 and 14 days). Gold concentrations in liver, spleen, kidney, heart, lung and brain were determined using inductively coupled plasma mass spectrometry (ICP-MS) and expressed as ng/mg tissue. The accumulation pattern and depletion profiles of AuNPs in different tissues could be quantitatively characterized using Cmax and AUC. The strength of this approach is that it can precisely determine the amounts of NMs in individual organs at a certain time point and can be used to calculate the percent of injected dose distributed to an organ at a specific time. The weakness is that it requires sacrificing a number of animals. A semi-quantitative approach can be used to assess the biodistribution of NMs in which NM concentrations in the organs and/or tumors are only evaluated by the strength of the fluorescent signal using a near-infrared reflection (NIR) fluorescence imaging system (Vats et al., 2017). The strength of this approach is it can be performed over multiple time points in the same living animals. The limitation is that only the relative distribution to different tissues is quantified, and not the absolute amounts of NMs deposited to individual organs. For example, Choi et al. applied NIR imaging method to investigate the distribution of quantum dots in multiple organs and found the strongest fluorescence signals in the bladder and liver for two types of

NPs (Choi et al., 2009). Therefore, this approach is not suitable to calculate the percent of injected dose to individual organs.

2.3. Lymphatic System

The lymphatic system plays an important role in the absorption and distribution of NMs from interstitium into lymphatic fluid, where NMs are further distributed to lymph nodes, associated lymphatic tissues (e.g., spleen and bone marrow), and then return to the blood (Li et al., 2017; Riviere, 2009). Following oral exposure, some NMs that evade preabsorption clearance pathways can enter both the blood and lymphatic systems by crossing the unstirred water layer and the epithelium of the gastrointestinal tract, though the oral bioavailability of NMs is generally low (e.g., 0.01%-5% for AuNPs and 0.01%-0.05% for TiO_2 NPs depending on the size and surface coating) (Li et al., 2010; Z. Lin et al., 2015; Yuan et al., 2019). Following subcutaneous, intramuscular, intradermal, and intraperitoneal injections, because of their large sizes, NMs are mainly absorbed through the highly permeable lymph vessels or via macrophages and subsequent cell trafficking into regional lymph nodes (Li et al., 2017; Yuan et al., 2019). Following a systemic intravenous injection, the concentrations of AuNPs in lymph nodes were overall higher than many other organs (e.g., lung, kidney, heart, testis, and brain), except liver and spleen, and this finding was consistent across different sizes of AuNPs (4, 13, and 100 nm), indicating extensive distribution of AuNPs to the lymphatic system (Cho et al., 2010).

2.4. Metabolism

The metabolism of NMs refers to the process that alters the original compositions and/or physicochemical properties of NMs, such as degradation, dissolution, drug release, aggregation, and opsonization (Yuan et al., 2019). Typically, metallic NPs are relatively stable and rarely metabolized, such as AuNPs (Z. Lin et al., 2015). Some NPs can be dissolved and then release their own ions, an example being AgNPs (Liu et al., 2012). Carbon nanotubes have been reported to undergo slow enzymatic degradation by oxidative enzymes (Vlasova et al., 2016). To increase their biocompatibility, metallic NPs can be coated with natural or synthesized polymers that can be cleaved off and subsequently degraded. To investigate the coating effects, the drug release efficiencies in different environments, such as changed pH, temperature, light, and different surface coatings were evaluated. For example, polydopamine was applied as the coating layer on doxorubicin-loaded mesoporous silica NPs to increase the sensitivity of nanodrug release to pH (Lei et al., 2019). When the pH became lower, the blocked drug molecules were released. In another example, the weakly acidic pH of the tumor extracellular matrix causes hydrolysis of boronic-ester bond between phenylboronic acid and dopamine, which leads to steady delivery and tumor-localized release of dopamine from mesoporous silicon NPs, an approach which significantly extends the half-life of dopamine as an angiogenesis inhibitor in antitumor treatment (Taleb et al., 2019).

2.5. Biocorona Formation

In terms of metabolism, a unique type of transformation which substantially affects TK of NMs is the formation of biomolecular coronas (mainly protein coronas), which has been discussed in many publications since it was proposed in 2007 (Cedervall et al., 2007).

Following intravenous injection, oral or inhalational exposure, different protein coronas can be formed immediately on the outer layer of NMs upon entering the blood circulation or upon contact with different biological fluids (Ortega et al., 2017; Shannahan, 2017; Walkey & Chan, 2012). Based on the relative affinity, protein coronas can be divided into hard and soft types (Garcia-Alvarez & Vallet-Regi, 2021). On the top of a hard corona, a soft protein corona or even protein clouds can form, which consist of low affinitive and rapidly exchanging highly complex layers of proteins (Figure 2) (Docter et al., 2015). Commonly adsorbed proteins include hemoglobin, fibrinogen, apolipoprotein, albumin, macroglobulin, and other proteins (Bai et al., 2021). In previous studies, multiple factors were found to be able to impact the composition of corona proteins, including NM type, size, shape, and surface charge. For example, using the magnetic separation method, the main hard corona proteins at the surface of positively charged superparamagnetic iron oxide NPs (SPIONs) include hemoglobin subunits beta-2 (16.76%), alpha-1/2 (16.50%), and beta-1 (13.04%), while those on negatively charged SPIONs mainly consisted of fibrinogen alpha chain (9%), beta chain (9%) and gamma chain (7%) (Sakulkhu et al., 2014). Unlike SPIONs, the most abundant corona protein was serum albumin for gold nanostars and nanorods (Garcia-Alvarez et al., 2018). For the gold nanostars, the total number of the identified adsorbed proteins were 406 and 215 for 40 nm and 70 nm, respectively, indicating a significant size-dependent effect (Garcia-Alvarez et al., 2018). Besides the metallic NPs, apolipoproteins were the most abundant proteins for liposomal NPs in the *in vivo* studies (Bai et al., 2021). Liposomal NPs could be modified with apolipoprotein E to significantly improve cellular uptake into the brain (Tamaru et al., 2014).

The formation of protein coronas has important impacts on the toxicokinetics of NMs, which in turn affects toxicity and risk assessment of NMs. On one hand, the accumulation of complement proteins, such as fibrinogen and opsonin, can accelerate the elimination of NPs upon recognition by the reticuloendothelial system (RES, also known as mononuclear phagocyte system [MPS]). For example, the plasma half-life of molecularly imprinted nanogels (i.e., the nanogel with the presence of human serum albumins) was twice of that of non-molecularly imprinted nanogels (Takeuchi et al., 2017). On the other hand, the formation of protein coronas with some other proteins, such as albumin and apolipoprotein, can prolong the blood circulation time of NPs. The half-life of albumin-coating poly(lactic-co-glycolic acid) (PLGA) NPs (PLGA@BSA NPs) can be two-fold of that for albumin-nonselective NPs in mice because PLGA@BSA NPs actively recruited endogenous albumin coronas to inhibit opsonic adsorption and complement activation, and subsequently recognition by the RES (Li et al., 2019).

Moreover, protein coronas may change tissue accumulation and tumor delivery rate of NPs. In the comparison of guaninerich (G-rich) oligonucleotides and poly-thymine (poly-T) oligonucleotide modified spherical nucleic acids (SNAs), Chinen et al. found G-rich SNAs adsorbed more proteins than poly-T SNAs both in types and amounts, which resulted in more accumulation of NPs in the liver and spleen (Chinen et al., 2017). On the contrary, Schäffler et al found that blood protein-conjugated NPs can enhance the delivery rate of brain and lung by reducing recognition by the RES (Schäffler et al., 2014).

Formation of protein coronas also impacts NM cellular uptake. In studies conducted with AgNPs in cultured keratinocytes, protein corona formation impacted extent of NM uptake (Monteiro-Riviere et al., 2013). Similarly, both surface coating and protein corona composition significantly affected tissue distribution of infused AuNPs in an isolated perfused tissue preparation (Riviere et al., 2018). Finally, surface coatings with resulting changes in biocorona protein composition modulated both cellular uptake and resulting cytotoxicity of AuNPs in cultured human endothelial cells, demonstrating their effects on both distribution and cellular toxicity (Chandran et al., 2017). Because of this phenomenon, some biofunctionalized complexes of protein coronas and NPs were synthesized for biomedical applications. PAS (proline, alanine, and serine) modified ferritin-based nanocarriers were found to reduce the formation of protein coronas and not activate complement C3 in mice (Tesarova et al., 2020). As a result, the delivery of cytostatic alkaloid ellipticine (Elli) with this nanocarrier (PAS-10-FRTElli) markedly reduced uptake by macrophages and enhanced the tumor delivery than Elli alone or unmodified FRTElli (Tesarova et al., 2020).

2.6. Elimination

Extensive work has been reported on the clearance pathways of various NMs. Upon entering the systemic circulation, NMs can be cleared through kidney/urine, biliary/fecal pathways, as well as being sequestered by the RES (Figure 3).

In the blood, uncoated bare NPs can be rapidly cleared by the RES, which leads to a half-life as short as a few hours (Hoshyar et al., 2016). The elimination half-life of NMs is usually evaluated through a blood or plasma PK or TK experiment. For example, Choi et al. (2011) treated BALB/c mice with AuNPs via a single IV injection. Blood was withdrawn at multiple time points to measure the gold content using ICP-MS. As a result, the half-lives of the NPs were calculated to be from 7 to 38 hours depending on their size, with plasma half-life inversely correlated to particle size. Many studies have found that the plasma half-life of NMs also depends on other factors, including surface modifications and targeting strategy (Z. Lin et al., 2015).

For hepatobiliary and renal clearance pathways, the NP size plays a key role. It was proposed in a quantum dot study that NPs smaller than 5 nm can be efficiently excreted in the urine; whereas quantum dots larger than 8 nm did not exhibit renal filtration, but uptake into the RES (Choi et al., 2007). The potential reason may be the limited functional or physiological pore size in the glomerulus. It is generally accepted that the key dimension in glomerular filtrate is the slit diaphragm which is approximately 43 nm (Longmire et al., 2008). However, considering the combined effects of glomerular capillary wall layers, the functional or physiological pore size may be significantly smaller and is approximately 4.5–5 nm (Longmire et al., 2008). Most studies monitor renal clearance by measuring NM excretion into the urine. In a study of gold nanoclusters modified with glutathione (GSH) and bovine serum albumin (BSA), the gold concentration and content were measured in mouse urine at multiple time points (Zhang et al., 2012). Since the average size of GSH-protected nanoclusters were 2.1 nm, they were rapidly excreted in the urine by 2 hours post-injection. In contrast, the BSA-protected nanoclusters with an average size of 8.2 nm

were not excreted by the kidney into the urine and instead accumulated predominantly in the liver.

If NMs cannot be cleared by the kidney, they may be processed in the liver and eliminated through bile into the feces. In a study of AuNPs with different sizes in female rats, the liver showed increased accumulation with increasing NP size (Hirn et al., 2011). To trace the elimination pathways of NPs in the animal body, some *in vivo* studies use fluorescence signals of dyes. Dai et al. (2014) used indocanine green (ICG), an FDA-approved tracer for hepatobiliary clearance, to examine the elimination of AuNPs. AuNPs (AF750-PEG-AuNPs) labeled with ICG were administered to BALB/c mice with a strong fluorescence signal observed in the first 4 hours post-injection in both the liver and intestine. Transmission electron microscopy (TEM) found liver accumulation of AuNPs with the gold core remaining completely in the hepatobiliary transit pathway. The results of elemental analysis by ICP-MS confirmed this result as AuNPs were detected in the feces over 14 days (Poon et al., 2019). It should be noted that the amount of NMs in the feces may be primarily due to hepatobiliary excretion if NMs are given through IV, but if NMs are given via oral administration, the amount in the feces is mainly due to unabsorbed fraction traveling through the gastrointestinal tract to be eliminated out via feces.

Besides these classical excretion routes, some aerosol-based NMs can be excreted through the lungs (Bose et al., 2014). Following intratracheal instillation, it was found that a significant amount (e.g., ~23% in this experiment) of AgNPs was removed from the lungs by mucociliary clearance, then swallowed by the animals into the gastrointestinal tract and then finally excreted via feces (Takenaka et al., 2001). Using radiotracer techniques, intratracheally instilled cerium dioxide (CeO_2) NPs were also found to be cleared via phagocytosis by alveolar macrophages in Wistar rats and subsequent removal through the tracheobronchial tree towards the larynx (He et al., 2010). Similar results were reported by Zhu et al. (2009) for 22 nm radioactive $^{59}Fe_2O_3$.

2.7. Challenges in Toxicokinetics

There are some limitations and challenges in existing reported TK studies of NMs. First, for blood and plasma TK studies, few studies compare the vascular elimination with tissue distribution in a granular enough time frame to integrate the processes into a single model. The major limitation of many of the existing TK studies for NMs are the limited sampling time points, which biases their calculated TK parameters purely based on experimental design and not the physical properties of the NM. For plasma TK studies, occasionally only 3 to 4 time points are collected and the data then analyzed using compartmental TK models (Poon et al., 2015; Roy et al., 2017). For tissue distribution studies, in some cases only 1 or 2 time points were sampled (Feng et al., 2021; Xu et al., 2020; Zang et al., 2019). This results in a strong bias for the calculated parameters to map onto the experimental time points collected. Sampling a limited number of time points may result in a dataset where all data points fall into the same distribution or elimination phase of the TK curve, which may consequently confound the calculation of the half-life of NMs. With such small sample times, there are not sufficient statistical degrees of freedom to solve complex multi-parameter TK models. Second, the data from *in vitro* assays, while useful

to calculate *in vitro* parameters such as cellular uptake rate, are of limited use to quantify the TK profile of NMs *in vivo* unless proper *in vitro* to *in vivo* extrapolation (IVIVE) is performed. The main issue of this challenge is the dosimetry consideration between *in vitro* and *in vivo* experimental designs. For *in vitro* systems, the administered dose of NMs (i.e., the equivalent nominal media concentration exposure) and the target cell dose (i.e., the delivered dose to the cell) are not equal, and they can vary significantly up to as high as three to six orders of magnitude depending on the extent of NM agglomeration, aggregation, sedimentation, and diffusion (Hinderliter et al., 2010). This challenge is even greater when different dose metrics are considered, i.e., for the same mass amount of a NM, the particle number and surface area could vary depending on the size of the NM. If the measured cellular dose or cellular content of NMs is not available, in silico computational models, such as ISDD or ISD3 can be used to predict the delivered dose to the cell based on the physicochemical properties of NMs, exposure conditions, and medium characteristics (Hinderliter et al., 2010; Thomas et al., 2018). Additionally, the nature of the protein corona formed *in vitro* is different as coronas are made up of cell culture protein constituents rather than those found in plasma *in vivo*. For *in vivo* testing, many physiochemical properties can affect NM biodistribution, such as Zeta potential, surface chemistry, agglomeration state, and size, which may subsequently have impacts on the delivered dose to the target organ (Teeguarden et al., 2007). Note that agglomeration state of NMs is an important factor influence the extent and mechanism of cellular uptake of NMs. For instance, caveolae-mediated endocytosis was the major pathway for well dispersed silica NPs, but micropinocytosis was the major pathway for agglomerated form of silica NPs (Halamoda-Kenzaoui et al., 2017). The exact impact of agglomeration state on the TK properties of different types of NMs remain to be investigated. Overall, it is a challenge to predict target organ exposure of different types of NMs following different routes of exposure and it is also a challenge to use *in vitro* dosimetry and toxicity data to inform *in vivo* TK profiles and toxicity assessment. The vast number of different types of NMs due to different physicochemical properties make these challenges even greater.

2.8. Physiologically Based Pharmacokinetic (PBPK) Models

One approach that may address the above-mentioned challenges in TK of NMs is physiologically based pharmacokinetic (PBPK) model. PBPK modeling is a mechanistic modeling approach that simulates the absorption, distribution, metabolism, and excretion of a chemical or a NM and/or the metabolites in the body based on real anatomical characteristics using mathematical algorithms (Fisher et al., 2020; Lin et al., 2017). PBPK models can describe TK behaviors of a substance in relation to species-specific and age-dependent physiological parameters (e.g., individual organs' blood flows, weights, enzyme expression and activity), exposure-specific information (e.g., exposure dose, route, interval and duration), and chemical-specific mechanisms, such as metabolic pathways, protein binding for small molecules and protein corona formation for NMs. Compared to traditional empirical TK models, the advantages of PBPK models are the ability to predict target organ dosimetry based on external dose following different routes of exposure and a great ability to extrapolate across species, exposure paradigms, and from *in vitro* to *in vivo*. Multiple PBPK models have been developed for different NMs (Utembe et al., 2020; Yuan et al., 2019), and some of existing models have been used to perform risk assessment, including AgNPs

(Bachler et al., 2013), TiO$_2$ NPs (Bachler, von Goetz, et al., 2015), and AuNPs (Cheng et al., 2018). Some studies have demonstrated that PBPK models can be used to perform NP IVIVE for kinetic (Bachler, Losert, et al., 2015) and toxicity data (Lin, Monteiro-Riviere, Kannan, et al., 2016). Recent studies have also shown that PBPK models can be used to predict delivery efficiency of NPs to tumors in tumor-bearing mice (Cheng et al., 2020; Lin et al., 2022). These models serve as a basis for extrapolating to humans to evaluate safety and risk of cancer nanomedicines in humans.

While PBPK models have the potential to address the challenges in TK studies of NMs, they also have their inherent shortcomings. First, compared to traditional empirical TK models, PBPK models are more complex and require more parameter values and thus more data to calibrate and evaluate. They require a greater amount of effort, expertise and resources to develop a PBPK model than needed for a simple but limited TK model. Second, most of existing PBPK models for NPs are built based on data from intravenous injection studies (Utembe et al., 2020; Yuan et al., 2019). PBPK models following other routes of exposure are needed as humans are often exposed to NMs following extravascular routes, such as dermal contact, and oral or inhalational exposure. Third, while many PBPK modeling approaches, such as IVIVE, route-to-route extrapolation, and interspecies extrapolation have been well established for small molecules, whether these approaches are applicable to NMs have not been systemically evaluated. A recent study showed that the traditional route-to-route extrapolation approach that is typically used for small molecules is not applicable to NMs because NMs form different types of protein coronas through contact with different biological fluids following different routes of exposure (Chou et al., 2022). Therefore, while PBPK modeling is useful for NMs, proper methodologies of PBPK modeling for NMs remain to be established.

2.9. Linkage of Toxicokinetics to Risk Assessment

In the field of toxicology, there is a fundamental tenet that it is the internal target organ dose, rather than the external exposure dose, that determines the adverse response of a xenobiotic. PBPK models are an important tool in chemical risk assessment in part because it can be used to predict internal target organ dose, thus linking TK to risk assessment. For small molecular chemicals, the external or internal dose metric is typically expressed as mass (e.g., mg or mM of a chemical per unit mass of liver). For NMs, the dose metrics could include mass, particle number, and surface area. For certain toxicity endpoints, such as lung inflammation, some studies have shown that the best dose metric for dose-response analysis may be the surface area (Oberdorster et al., 2007; Schmid & Stoeger, 2016) or the particle number (Wittmaack, 2007). Whether the surface area or the particle number may be the best dose metric for other toxicity endpoints (e.g., cell death) remains to be investigated. Currently, almost all PBPK models for NMs are based on the dose metric of mass partly because existing NM PBPK models were built based on the PBPK modeling approaches that were established for small molecules (Utembe et al., 2020; Yuan et al., 2019). Existing PBPK-based studies extrapolating dosimetry and toxicity data from *in vitro* to *in vivo* are also based on the dose metric of mass (Cheng et al., 2018; Dubaj et al., 2022). This is appropriate considering that a PBPK model is designed to be able to predict internal doses of several target organs and then to assess the dose-response relationships of different

toxicity endpoints. In fact, the use of the dose metric of mass in PBPK models is desirable because it allows to account for the maximum uptake capacity in a cell or tissue, which is important in the TK of NMs. The use of surface area or particle number is less favorable to account for the maximum cellular or tissue uptake capacity because these dose metrics are highly depending on the particle size. However, since surface area or particle number may be a better dose metric to describe lung inflammation, it may be worth to explore PBPK modeling approaches based on these dose metrics.

3. RISK ASSESSMENT

Depending on the size, particulate matter (PM) can be classified into coarse particles (PM_{10}, particles 10 μm in diameter), fine particles ($PM_{2.5}$, particles 2.5 μm in diameter), and ultrafine particles ($PM_{0.1}$, particles 0.1 μm in diameter), including engineered NPs. The methodology for risk assessment of coarse particles, fine particles, and environmental chemicals has been well established, and consists of four steps, including hazard identification, dose-response assessment, exposure assessment and risk characterization (EPA, 2010, 2014; Kimmel et al., 1999). For risk assessment of NMs, the guidance is just beginning to be established (EFSA, 2021), and it is mainly based on the guidance that has been established for larger coarse and fine PM (EPA, 2010). Therefore, in general, risk assessment of NMs also follow the same steps used for fine particles and environmental chemicals. However, compared to coarse and fine particles, it is generally considered that NPs have a higher toxicity because they are much smaller and can penetrate deep into the lung and be translocated throughout other parts of the body, and also NPs have a much larger surface area and number of particles compared to coarse and fine particles for the same given mass dose (Kumar et al., 2021; Schraufnagel, 2020). As such, the human health guidance values for the same chemical substance but with different sizes could be different. For example, the National Institute for Occupational Safety and Health (NIOSH) recommends an airborne exposure limit of 2.4 mg/m^3 for fine TiO_2, but recommend a much lower value of 0.3 mg/m^3 for ultrafine TiO_2, including engineered nanoscale TiO_2 (NIOSH, 2011). Therefore, one needs to pay particular attention to the unique physicochemical properties of NMs in the risk assessment process.

3.1. Hazard Identification

Toxicities of various NMs have been evaluated using different approaches under different experimental settings. The degree of toxicity of a particular NM depends on the extent of exposure and its physicochemical properties, as well as the sensitivity of the test organism. To compare the toxicity of different types of NMs, a group of scientists from Netherlands evaluated the toxicities of multiple types of NMs and classified the hazard of different NMs into four classes based on their respective nano reference values, including class 1 high toxicity with a nano reference value of 0.01 fibers cm^{-3} for rigid carbon nanofibers and metal oxide fibers (e.g., SWCNT), class 2 medium or low toxicity with a nano reference value of 20,000 particles cm^{-3} for granular NM (non-fibrous), stable in the environment, with a density >6 g cm^{-3} (e.g., Ag and CeO_2 NPs), and class 3 medium or low toxicity with a nano reference value of 40,000 particles cm^{-3} for granular NM and nanofibers, stable in the environment with a density <6 g cm^{-3} (e.g., TiO_2 and ZnO NPs), and class 4 low toxicity

for granular NMs, unstable or soluble in water (e.g., NaCl and lipid NPs) (Van Broekhuizen et al., 2012; Włodarczyk & Kwarciak-Kozłowska, 2021).

Chemical risk assessment starts with a hazard assessment. The hazard of NMs can be evaluated in various ways, including *in vitro*, *in vivo* animal, and human epidemiological approaches. Traditionally, hazard identification is based on high dose exposure in short- and long-term animal bioassays, as well as epidemiological studies. However, within the framework of the toxicity testing in the 21st century (Tox21) program, non-animal-based new approaches methodologies, including *in vitro* assays, are increasingly used. For the rest of this section, we will summarize toxicity assessment of NMs using *in vivo* animal assays, human epidemiological studies, and *in vitro* assays, respectively.

The animal bioassays on NMs were conducted with different exposure durations. For TiO_2, the National Toxicology Program conducted a 2-year oral carcinogenicity bioassay in which F344 rats and B6C3F1 mice of both sexes were fed with diet containing TiO_2 at 0, 25000, and 50000 ppm for 103 weeks (NTP, 1979). Although the study concluded that no carcinogenicity was found, some non-neoplastic effects were reported, such as congestion and hemorrhage in lung, fibrosis in the heart, hyperplasia of the bile duct, atrophy of the seminal vesicles, and galactocele formation in the mammary gland. For TiO_2 or other types of NPs, standard 2-year carcinogenicity bioassays have not been reported. To investigate the non-neoplastic effects, subchronic studies are more commonly used, which range from 14 to 90 days. The organ system toxicity of TiO_2 NPs were studied following 30-day repeated oral exposure in young and adult rats (Wang et al., 2013). Liver edema, including hepatic cord disarray, perilobular cell swelling, vacuolization or hydropic degeneration, was found in the young rats at 50 and 200 mg/kg dose levels; whereas in adult rats the symptom of liver edema did not occur and only inflammatory cell infiltration was observed in liver of adults rats in 10 and 50 mg/kg dose groups (Wang et al., 2013). Another study investigated possible toxic effects on reproductive and endocrine systems of short-term oral exposure to anatase TiO_2 NPs (0, 1, 2 mg/kg/day for 5 days) via drinking water in Sprague-Dawley rats (Tassinari et al., 2014). The study found histopathological changes in thyroid, adrenal and ovary, as well as increased testosterone in serum of male rats, but decreased testosterone concentrations in female rats. Similar toxicology studies were conducted for AgNPs (Braakhuis et al., 2014; Garcia et al., 2016; Ji et al., 2007; Sung et al., 2008; Vandebriel et al., 2014), quantum dots (Hauck et al., 2010; G. Lin et al., 2015), and other NMs using rodents of different ages as it is important to understand NM hazards on different life stages.

Unlike environmental chemicals, the unique effects of agglomeration and aggregation of NMs can significantly alter their toxicological responses *in vitro* and *in vivo*. The term of agglomeration is used to describe the phenomenon that NMs are associated into a loose cluster that can be simply broken down by mechanical forces (reversible); whereas aggregation refers to NMs forming a strong, dense, and stable particle collective (irreversible). Agglomeration and aggregation will markedly influence the toxicological effects of NMs both *in vitro* and *in vivo*. The impact is particularly prominent at a high dose exposure study as the concentrations of NMs are often so high that most particles either agglomerate or aggregate, resulting a larger size of NMs that are absorbed to a lesser extent,

thereby changing their toxicity. In general, NMs with a smaller agglomerate size of the same material are distributed more extensively to more organs, resulting in a higher accumulation in some organs with greater toxicity (Balasubramanian et al., 2013). In inhalational studies of TiO2 NPs, small agglomerates (<100 nm) caused greater cytotoxicity and oxidative stress effects in rats' bronchoalveolar lavage fluids (BALF) than large agglomerates (>100 nm) (Noël et al., 2013; Noël et al., 2012). It was hypothesized that small agglomerates may escape the first defense mechanism of pulmonary clearance via macrophage phagocytosis, and thus are more likely to interact directly with biological materials, resulting in greater toxicity than large agglomerates. During *in vitro* testing, the agglomerates may impact the cell-particle interactions due to the altered size and shape (Kong et al., 2011). In a cytotoxicity and genotoxicity *in vitro* study, TiO_2 NPs with less dispersion and larger agglomerates were found to cause greater DNA oxidation lesions and DNA damage for human and primate cells than those with agglomerates less than 200 nm (Magdolenova et al., 2012).

The health hazards of NMs in humans were also investigated in epidemiological studies, including cohort studies and clinical trials. For example, a clinical trial investigated the relationship between occupational exposure to airborne unintentionally released NPs and the lung burden of NPs in patients' BLAF and lung diseases (Forest et al., 2021). The results suggested that the occupational inhalation of airborne NPs potentially contributed to the development or exacerbation of lung diseases. In the ceramic industry, a few studies have shown that occupational exposure to ceramic dusts and fibres is associated with various lung diseases, including chronic bronchitis, chronic obstructive pulmonary disease, reduced lung function, wheezing, breathlessness, and dry cough. However, because the ceramic dusts and fibres were of different sizes with different raw materials such as carbon-, metal-, and metal oxide-based fine particles or NPs, it is unknown whether a specific type of NPs may cause a specific type of lung diseases.

There are also studies investigating NM toxicity using *in vitro* experiments. Common *in vitro* assays include cellular interaction, viability, apoptosis, oxidative stress/inflammation and endotoxin assays (Savage et al., 2019). For example, an *in vitro* study found that AuNPs coated with branched polyethylenimine (BPEI) caused time- and concentration-dependent increase in reactive oxidative stress in human primary hepatocytes, but when BPEI-AuNPs were pre-coated with human plasma protein corona, it substantially reduced reactive oxidative stress in hepatocytes (Choi et al., 2017). The results of *in vitro* toxicity assays may be differed due to various NM physicochemical properties, such as the size, surface coating, biocorona formation, etc. In the study of AgNPs uptake in human epidermal keratinocyte, pre-incubation of cells with immunoglobulin G for 2 h remarkably reduced cellular uptake of 110 nm citrate AgNP, but resulted in the greatest uptake for 20 nm silica-coated AgNPs. In contrast, pre-exposure of transferrin to the cells enhanced the uptake of 120 nm silica-coated AgNPs (Monteiro-Riviere et al., 2013).

For NM *in vitro* cytotoxicity assays, it is important to note that there are a variety of cytotoxicity assays, and it has been shown that some classical dye-based assays, such as MTT and neutral red may produce invalid results due to NM/dye interactions and/or NM adsorption of the dye/dye products (Monteiro-Riviere et al., 2009). In this study, human

epidermal keratinocytes (HEK) were exposed to different NMs (carbon black, single-walled carbon nanotubes, fullerenes, and quantum dots), and cell viability was evaluated with different assays, including calcein AM Live/Dead, neutral red, MTT, Celltiter 96 AQueous One, alamar Blue, Celltiter-Blue, CytoTox Onetrade mark, and flow cytometry. Results from the assays that depend on direct staining of live and/or dead cells (trypan blue, Live/Dead, and calcein AM) were variable and difficult to interpret due to physical interference of NMs with cells; and results from the dye-based assays (MTT and neutral red) also varied greatly, depending on the interactions of the dye/dye products with NMs). This study suggests that some cell viability assays may not be suitable for evaluating NM cytotoxicity, and it is recommended that more than one assay is needed when determining NM cytotoxicity for risk assessment (Monteiro-Riviere et al., 2009).

Traditionally, animal testing is used as the gold standard for toxicity evaluation and the human health risk assessment relies almost exclusively on *in vivo* results (Blaauboer & Andersen, 2007). However, in 2007, the National Academies of Science published a landmark report on toxicity testing in the 21st century (NRC, 2007). In this report, the goal of future toxicity testing is to transition from the current lengthy and expensive animal bioassays to *in vitro* assays coupled with *in silico* computational modeling. Since that time, multiple federal agencies have been working collaboratively on the Tox21 program that results in a large amount of *in vitro* assay data on hundreds of endpoints for thousands of chemicals (Richard et al., 2021). In 2013, European Union banned animal testing for cosmetic ingredients (EU, 2013). In 2019, US EPA announced that they plan to substantially reduce animal testing on mammals by 30% by 2025 and eliminate it by 2035 (EPA, 2019). Similarly, in 2021, Mexico announced to ban animal toxicity testing for cosmetics (HSI, 2021). Therefore, it is anticipated that *in vitro* toxicity assays coupled with *in silico* modeling will be increasingly used in future hazard identification and risk assessment studies of both environmental chemicals and NMs.

One challenge of the *in vitro* assays is the validity of the in *vitro* test system and how to extrapolate the results to *in vivo*. There are several issues that may cause false negative and/or false positive effects in the *in vitro* test system, including high-dose effects, time-course effects, and cell line effects. Specifically, *in vitro* studies are usually conducted with a high-dose and short-term exposure. However, some effects may only be detected at a high dose *in vitro* that may not be applicable to *in vivo* scenarios where the exposure dose is usually relatively low and thus cannot be directly extrapolated to low-dose effects *in vivo*. Moreover, the design of a high-dose exposure experiment for NMs may encounter the problem of solubility and agglomeration/aggregation issues discussed above, which subsequently alters the physicochemical properties of the NMs and their toxicological effects. As a result, the physicochemical properties of the NMs evaluated in the *in vitro* test system are no longer the same as those evaluated in the *in vivo* test system. Also, in a short-term *in vitro* study, the observed effects may be temporary (e.g., release of inflammatory mediates and cell proliferation) and are difficult to predict the toxicological effects observed *in vivo*, which usually after a long-term low-dose exposure. Additionally, toxicological effects may differ between different cells (e.g., liver vs kidney cells), different cell types (e.g., primary vs immortalized cells), and different stages of cells (e.g., undifferentiated, differentiating, and differentiated cells). The use of different types of cells requires different

culture mediums and may form different protein coronas, which will also confound the hazard identification of NMs *in vitro*, creating a challenge to extrapolate the results to *in vivo* (Lai, 2012).

Another challenge in the hazard assessment of NMs is insufficient understanding of long-term toxicity of NMs, along with inadequate data of dose-response relationships between NM exposure and the adverse health effects in animals and humans. With the rapid advancement of nanotechnology, NMs can be synthesized with different physicochemical properties, resulting in different toxicities. The current animal bioassay approach cannot keep pace with the rapid increase in the number of different types of NMs. Additionally, while many *in vitro* assays are available, most *in vitro* assays have been evaluated with environmental chemicals only, but not with NMs, and as introduced above, some *in vitro* assays may not be applicable to NMs and the approach to extrapolate *in vitro* toxicity of NMs to *in vivo* has yet to be established. When being in contact with biological matrices, NMs may undergo modifications, such as protein corona formation, agglomeration, dissolution, and interaction with other particles. These transformations can interfere with the toxicological effects observed with NMs (Ortega et al., 2017). Such issues are usually not fully considered during *in vitro* testing. All of these challenges introduce great uncertainties in the risk assessment of NMs and thus slow down the risk assessment process. Therefore, toxicity testing of NMs is under increasing pressure to meet the competing demand of testing a large number of new NMs introduced into commerce, evaluating potential adverse effects with respect to all critical endpoints and life stages, and reduce animal use and cost (Krewski et al., 2010).

3.2. Dose-Response Assessment

The dose-response assessment is the second step in the risk assessment of environmental chemicals and NMs. Dose-response assessment describes how the likelihood and severity of the adverse effects are related to the exposure dose. Originally, the dose-response relationship as expressed using the lethal dose for 50% of the animals (i.e., LD_{50}) or the half-maximal effective concentration (EC_{50}). This method is very robust for small aquatic animal studies, such as daphnia and zebrafish in ecological risk assessment. For example, Li et al exposed *Portunus trituberculatus* to copper oxide (CuO) NPs in seawater for 96 hours and determined the LD_{50} to be 49 mg/L (Li et al., 2021). However, LD_{50} is not ethical from an animal welfare perspective, and is not typically used for human health risk assessment. To assess the dose-response relationship for human hazards, the dose-response assessment for environmental chemicals or NMs can be performed using two methods: a traditional approach to determine the No Observed Adverse Effect Level (NOAEL) and/or the Lowest Observed Adverse Effect Level (LOAEL) or a newer approach to calculate the benchmark dose (BMD).

NOAEL refers to the highest dose at which no adverse effects have been found, while LOAEL is the lowest dose at which significant adverse effects were observed (EPA, 2012). NOAEL is usually used as the point of departure (POD) for extrapolation from animal toxicity results to humans. NOAEL/LOAEL are commonly evaluated in animal toxicity studies of NMs. For example, the NOAEL of TiO_2 NPs was derived as 1000 mg/kg/day

for systematic toxicity in a subchronic study in Sprague-Dawley rats (Heo et al., 2020). In another subchronic study, Wistar rats were fed with yitrium oxide (Y_2O_3) NPs at 0, 30, 120, and 480 mg/kg/day. Based on the significant histopathological changes and biochemical alterations at 120 and 480 mg/kg/day, the NOAEL of was identified as 30 mg/kg/day in Wistar rats (Panyala et al., 2019).

In 1984, Crump proposed the benchmark dose (BMD) approach as an alternative of the NOAEL/LOAEL approach (Crump, 1984). The objective of the BMD analysis is to identify the best model for the collected dose-response data, and then to determine the BMD dose that results in a predefined response (e.g., 5%, 10% and 20%) compared to the control group (EPA, 2012). Briefly, the general procedure in a BMD calculation includes selecting appropriate models based on the data type, fitting the dose–response data, evaluating the goodness of fit of the models, selecting a benchmark response (BMR), calculating the BMD and its lower bound (BMDL), and deciding the final values of the BMD and BMDL from the models that are able to fit the data adequately (Chen, 2020). If multiple models are acceptable to describe the dose-response data, then the BMD value from the best model can be selected or the average BMD based on all BMD values of all acceptable models can also be used. Representative dose-response studies of NMs using the BMD approach are listed in Table 2.

Multiple software programs are available for BMD calculations to meet various research needs, such as PROAST from National Institute for Public Health and the Environment of Netherland, BMDS from US EPA, and BMDExpress (Sciome LLC, Research Triangle Park, NC). Using the PROAST software, the cytotoxicity of CuO NPs was evaluated in Caco-2 cells and mouse macrophage cells, and the calculated BMD_{20} were 4.44 $\mu g/cm^2$ in Caco-2 cells (Ude et al., 2017) and ranged from 2.06 to 55.6 $\mu g/mL$ depending on the surface coatings in mouse macrophages (Libalova et al., 2018). The dose-response relationship of *in vivo* toxicity of CuO NPs was also assessed using the PROAST software. The BMD_{20} values were calculated for the changes of organ weight and clinical chemistry after 7 days of exposure, and the lowest BMD was found to be 26.2 mg/kg for the change of serum liver enzyme aspartate aminotransferase (AST, an indication of liver toxicity) (De Jong et al., 2019). In an *in vitro* study using lung cells, the toxicity of multiple NPs, including CeO_2, CuO, TiO_2, ZnO, and ZrO_2 (zirconium dioxide), were ranked based on the lowest BMD among multiple cellular endpoints, and the study showed that the toxicity decreased in the following order: $ZnO > CuO > TiO_2 > ZrO_2 > CeO_2$ (Pink et al., 2020). In a secondary analysis of quantum dot NM using *in vivo* and *in vitro* toxicity data, a linear dose-response model was used to compare the adverse effect using cytokine level changes in different mouse strains (Weldon et al., 2018). This study showed consistent responses in common endpoints (e.g., cytotoxicity, pro-inflammatory responses, and strain sensitivity) between *in vitro* and *in vivo* studies. This study suggests BMD analysis can be used as an effective tool to compare sensitivity of different strains, cell types, and assays.

Compared to the BMD approach, the limitations of the traditional NOAEL/LOAEL approach are well known and have been discussed in many studies (Crump, 1984; EPA, 2012). The most notable one is that the NOAEL/LOAEL approach is highly dependent on the study design, such as dose selection and sample size because NOAEL/LOAEL is limited

to one of the experimental doses. Inappropriate dose selection or lack of understanding of the NM toxicity can lead to the failure to find the threshold for NM's safe use. For example, in a subchronic study using Sprague Dawley rats, the NOAEL for agglomerated/aggregated TiO_2 NPs (~180 nm) was determined as the highest experimental dose of 1000 mg/kg/day because no systemic toxicological effects were found after all clinical pathology, necropsy, and histopathological examinations (Heo et al., 2020). However, such results may substantially differ from other studies depending on the dose selection, toxicity endpoint, and type of NPs. Another 30-day oral gavage study identified a NOAEL of 62.5 mg/kg/day for 5 nm anatase TiO_2 NPs in female CD-1 mice (Duan et al., 2010). Sufficient understanding of the toxicity of a particular NM and well-organized dose spacing are critical to derive the NOAEL and LOAEL of NMs. Moreover, the variability and uncertainty of the experimental results are not taken into account using the NOAEL/LOAEL approach. As only a limited number of animals can be tested in a typical dose-response experiment, the uncertainty of the mean responses is obviously great. Therefore, a better way for dose-response data analysis is to consider the confidence intervals instead of the exact mean value (EFSA, 2011). Additionally, the NOAELs derived from different studies are difficult to compare due to different dose selections and study designs.

The BMD method is preferable by many regulatory organizations because (1) it takes data at all doses into account so that the background response can be considered rather than assuming it to be zero, (2) the derived toxicity values are easy to be compared among different studies and data types, and (3) it can better account for statistical uncertainty and variability (Haber et al., 2018; Shao et al., 2019). In 2012, U.S. EPA published technical guidance for BMD analysis (EPA, 2012). In 2017, the European Food Safety Authority (EFSA) Scientific Committee reconfirmed that the BMD method is a scientifically more advanced approach for chemical dose-response assessment and recommended it for chemical risk assessment (EFSA et al., 2017).

Besides the different choices of dose-response analysis method, there are also some challenges in the dose-response analysis of NMs. First, the target organ dosimetry is difficult to determine or predict. The elemental composition of different NMs and their properties, such as surface area, tendency to aggregate, interaction with cells, are completely different for different types of NMs (Hegde et al., 2016). For different NMs, the same administered dose may result in quite different target organ dosimetry, and thus different dose-response relationships. During *in vitro* testing, some unique *in vivo* transformations, including protein corona formation and spontaneous agglomeration, are rarely considered, which may impact the relevance of *in vitro* NM dose-response profiles to *in vivo* conditions (Teeguarden et al., 2007). Consequently, the use of *in vitro* data for dose-response modeling is limited. As the toxicological effects of NMs are assessed in more *in vitro* studies than the environmental chemicals, this issue becomes more significant for the dose-response assessment of NMs. Some previous studies developed *in silico* models to predict the impact of protein corona formation on TK of NMs during interspecies extrapolation. For example, a NP biodistribution model was developed to assess the influence of differential biocorona formation kinetics on anticipated tissue distribution across rodent-to-human extrapolation (Sahneh et al., 2015). This study found that although NMs can successfully reach target organs in rodents, the target organ dosimetry may be quite different in humans due to

different biocorona formation kinetics between species (i.e., the longer circulation time allows for further biocorona evolution in humans).

Second, the selections of critical effects in most of current dose-response analyses of NMs are ambiguous and lack full justification. For *in vivo* studies, the dose-response analyses are usually conducted for all plausible changes in organ weights, clinical and other effects (De Jong et al., 2019; Gosens et al., 2015). However, these studies rarely identify the critical effect for a particular NM. One reason for this deficit could be the lack of a robust body of scientific evidence defining NM hazards. In BMD analysis, BMR refers to a predetermined change from the control value. The selection of BMR involves the judgments about the statistical and biological characteristics of the datasets. The U.S. EPA recommended 10% extra risk and a change of one control standard deviation as the BMR for standard reporting for dichotomous and continuous data, respectively (EPA, 2012). In the *in vitro* study of CuO NPs, the BMR was selected as 20% relative change of cytotoxic endpoints (Libalova et al., 2018). In another study of AgNPs, the BMR was determined as 5% for immunotoxicity (Vandebriel et al., 2014). Consequently, the comparability and significance of such results are decreased.

It is also important to note that not all NM toxicity data can be fitted by existing BMD or biologically-based models (EPA, 2012). For example, following exposure to a high dose of NPs, some NPs may not be soluble due to the large dose and eventually aggregate or agglomerate, resulting in reduced bioavailability or leading to local effects that are purely due to dose-induced aggregation/agglomeration. These high-dose effects may be quite different from low-dose effects, and cannot be described with existing BMD models. One of the solutions is to drop the data of the highest dose. Considering the limitations of the BMD method, it is still necessary to use the NOAEL/LOAEL approach when the BMD method is not applicable.

3.3. Exposure Assessment

Exposure assessment refers to the process of characterizing, estimating, measuring and modeling the frequency, duration, and magnitude of contact with a chemical, including external exposure or administered dose and internal dose to individual organs (Peters et al., 2016). For conventional environmental chemicals, many studies have been conducted for exposure assessment and some standard methods have been used. Some of these methods have been applied in the nanotechnology industry.

For NMs that have been employed in certain industries, regulatory agencies have published detailed exposure assessment reports. For example, TiO_2 NPs are commonly used in cosmetic products, including make-up, sun screens, hair, skin and oral care products as it is component of mineral cosmetics (Włodarczyk & Kwarciak-Kozłowska, 2021). To evaluate their safety, the Scientific Committee on Consumer Safety (SCCS) in the European Commission conducted an inhalation exposure assessment for pressurized cosmetic aerosols, pump sprays and cosmetic powders containing TiO_2 NPs. In this evaluation, the lung exposure was measured from the field inhalation exposure study, including the dosage for each application of different types of the products (i.e., spray or loose powder), number of applications for each day, and the TiO_2 concentration in each formulation. As a result, the

thoracic fractions of inhaled TiO_2 dose were 125 and 10.35 μg/day for hair styling spray and loose powder, respectively. Accordingly, the SCCS concluded that the use of pigmentary TiO_2 NPs in a hair styling spray is safe under a maximum concentration of 1.4% for general consumers, and 1.1% for hairdressers (SCCS, 2020).

The exposure of NMs have also been assessed in food products. As TiO_2 NPs are also widely used in food industry (food-grade TiO_2, E171), human exposure through food was measured as the product of the concentration of TiO_2 NPs in each type of food times the intake amount of each food product (Weir et al., 2012). The results suggested 1–2 mg/kg/day for US children under 10 years old, and 0.2–0.7 mg/kg/day for the people in other age groups.

For occupational exposure, multiple guidelines of NMs have been published. In 2010, the British Standard Institution published "Guide to assessing airborne exposure in occupational settings relevant to nanomaterials" (BSI, 2010). In 2017, the Organization for Economic Co-operation and Development (OECD) published "Strategies, techniques and sampling protocol for determining the concentration of manufactured nanomaterials in air at the workplace" (OECD, 2017). In the manufacture setting of TiO_2 NPs, a study evaluated NM exposure among workers by the assessment of the surface area concentration in the trachea and bronchi coupled to questionnaire data collection. The results showed a significant higher surface area concentration of TiO_2 in the NP-exposed workers and associated alteration of clinical chemistry compared to the non-exposed control group (Xu et al., 2016). Moreover, exposure assessment of NMs can be conducted to measure the surface area concentration, particle number and the mass concentration using analytical instruments. For example, a generic exposure concentration profile was measured every 15 minutes in the breathing zone of workers over a work shift. In 7 hours, a time-concentration exposure curve was generated, which can be compared with time-weighted average occupational exposure limits and short-term exposure limits (Peters et al., 2016).

To better protect worker safety, several occupational exposure limits have been established for some NMs (Table 3). In the case of TiO_2 NPs, the International Agency for Research on Cancer (IARC) in 2010 reviewed the evidence of TiO_2 hazards and concluded it as a possible carcinogen to humans. Governments and some organizations subsequently established workplace exposure limits (WEL) for TiO_2, including 15 mg/m^3 averaged over an 8-hour work shift by the U.S. Occupational Safety and Health Administration (OSHA) (OSHA, 2021), 2.4 mg/m^3 for fine size and 0.3 mg/m^3 for ultrafine size (including engineered nanoscale) averaged over a 10-hour work shift by NIOSH (NIOSH, 2011), and 10 mg/m^3 averaged over an 8-hour work shift by the American Conference of Governmental Industrial Hygienists (ACGIH) (ACGIH, 2021). In another instance, the exposure to respirable carbon nanotubes was limited to 1.0 μg/m^3 as an 8-hour time-weighted average based on the NIOSH guidance (NIOSH, 2013).

Unlike conventional chemicals for which multiple standards have been applied to measuring and reporting the exposure, a standard method for NMs has not been established. The existing methods may or may not be suitable for NMs due to the small particle size and large surface area which results in significantly different effects than that seen with individual

organic molecules. (Zhao & Zhang, 2019). For engineered NMs, there is no consensus on the optimal sampling methods to assess their exposures resulting in data gained of low comparability and reproducibility. Another important issue is that NMs in actual use and actual exposure may not be the same as the form/degree of agglomeration in the test materials in a laboratory study. Moreover, due to the lack of sufficient understanding of the hazards of NMs qualitatively and quantitatively, the results of exposure assessment of NMs are difficult to be fully used in the risk assessment of NMs.

3.4. Risk Characterization

Risk characterization is a process that synthesizes and summarizes all the information from hazard identification, dose-response analysis, and exposure assessment, as well as other relevant information. The output of risk characterization is an overall quantitative assessment (and if not possible qualitative) on the safety of a substance (either a conventional chemical or a NM) in its intended use together with parameters under which the assessment is valid and the uncertainties associated with the assessment (EFSA, 2021). Specifically, a critical effect is identified at the hazard identification step; a POD is determined at the dose-response assessment stage; a human equivalent dose is calculated based on the POD from *in vitro* or *in vivo* toxicity studies; and then the reference dose on the safe use or safe exposure of the substance can be derived by considering necessary uncertainty factors (Cheng et al., 2018; Chou & Lin, 2021). The uncertainty factors include 10 to account for intraspecies variability, 10 for interspecies uncertainty, 10 for subchronic-to-chronic extrapolation, 10 for LOAEL to NOAEL extrapolation, and 10 for an incomplete database for U.S. EPA (Dourson et al., 1996). Note that different regulatory agencies have slightly different guidelines on uncertainty factors (Dourson et al., 2022; Dourson et al., 1996). According to the latest guidance on risk assessment of NMs to be applied in food and feed chain (EFSA, 2021), risk characterization of a NM considers the same elements as for conventional environmental chemicals, and if the available data have been derived from appropriately conducted studies using validated methods and NM-specific factors have been considered, then it does not need to use higher uncertainty factors for a NM than for a conventional material or a chemical. However, if the data are insufficient or the data have been generated from inadequate tests or using invalid methods for NPs, then applying additional or higher uncertainty factors may be needed for conservative risk characterization.

4. FUTURE PERSPECTIVES and CONCLUSION

In conclusion, ongoing efforts in the risk assessment of NMs are valuable and need to be continued as more and varied NMs are developed. Based on our current knowledge, risk assessment of NMs is more complicated than environmental chemicals as the toxicity of NMs can be impacted by many additional factors (e.g., size, shape, Zeta potential, surface coating, extent of agglomeration/aggregation, protein corona formation, etc.) and the methodologies for identification of critical effects, extrapolation of TK and toxicity data from *in vitro* to *in vivo* and across species, have not been well established for NMs. Additional studies on TK, toxicity, and PBPK are warranted, especially on how to extrapolate TK and toxicity data from *in vitro* to *in vivo* and from animals to humans.

Considering the above-mentioned challenges, the following considerations should be taken into account when designing future TK, toxicity, dose-response, PBPK, and risk assessment studies for NMs.

TK studies of NMs can benefit both the understanding of NM toxicity and relevant risk assessment by better defining the relationship of external dose and length of exposure with subsequent tissue distribution and ultimately toxicological effects. For plasma TK studies, it is important to sample enough time points at appropriately distributed intervals to capture the entire kinetic profile from the absorption (if extravascular administration) to elimination phases, and have enough time points (at an absolute minimum 3) at the elimination phase to calculate the terminal elimination rate constant, which is needed to calculate the elimination half-life. The sampling time points also need to consider the species, study objective, sampling strategy, available resources, etc. Readers are referred to a detailed guidance by Valic et al. on the TK study design of NMs (Valic et al., 2020).

For biodistribution studies, it is often not practical for the number of sampling time points to be as many as plasma TK studies due to limited availability of animals and animal welfare considerations. In this case, the sampling plan should consider the study objective. For example, if the objective is to evaluate the efficacy of a NM or a NM-carried drug, then the sampling time points should focus on the earlier kinetic phase in order to capture Cmax and possibly Ka. If the study objective is to collect tissue depletion data in order to build a PBPK model for risk assessment, then the sampling time points should focus more on the terminal elimination phase, so that the time for NMs to be depleted to be below a safe concentration or be excreted out of the body can be estimated.

For toxicity and dose-response studies, it is important to acknowledge the differences between *in vitro* and *in vivo* test systems and experimental designs (e.g., dose, length, media composition). Whenever possible, primary human cells from target tissues, such as liver and kidney should be used in the *in vitro* toxicity studies as these cells are closer to human *in vivo* conditions than are rodent or immortalized cells. For both *in vitro* and *in vivo* toxicity studies, sufficient number of concentration or dose groups (3 treatment groups plus a vehicle control group) should be used in order for the data to be suitable for dose-response analysis. Unrealistic high dose groups should not be used to avoid irrelevant toxicity results resulting from high-dose-induced agglomeration/aggregation. When extrapolating *in vitro* toxicity findings to *in vivo*, it is important to derive POD based on the target cell dose, which can be estimated using the ISDD or ISD3 model based on the administered dose, NP's physicochemical properties, and study design. When possible, human equivalent dose should be calculated based on target organ dose that is directly associated with the POD at the target cell *in vitro*.

When performing IVIVE and animal-to-human extrapolation, a PBPK model could be quite useful. A major use of PBPK models is their ability to integrate data collected using different experimental designs (doses, sample collection times, samples analyzed, etc.) and then using such models to predict toxicological effects (Cheng et al., 2020). However, PBPK-based route-to-route extrapolation, IVIVE, and animal-to-human extrapolation approaches for NMs remain to be systemically evaluated and established. Existing TK

studies in animals are mostly based on different types of NMs from different laboratories using different measurement methods, and human data are quite limited. Additional studies using the same type of NMs (and synthesized using the same techniques) to evaluate TK following different routes of exposure in animals and humans, and to determine resulting kinetic parameters *in vitro* such as uptake rates in different types of cells, are needed in order to evaluate and establish the proper methodology for NM PBPK analyses. Protein corona formation is an important feature in TK, toxicity, and risk assessment of NMs. Methodology of incorporating protein corona kinetics into a PBPK model remains to be developed, yet is paramount in order to fully leverage the advantages of PBPK modeling in exposure and risk assessment.

Finally, while challenges still exist, significant efforts on TK, toxicity, dose-response, and risk assessment studies on NMs in the past two decades have greatly improved our understanding of the potential risk of NMs. Based on these previous efforts, some regulatory agencies have published guidelines on risk assessment of NMs in food and feed (ANSES, 2021; EFSA, 2021). Additional studies by considering the abovementioned data gaps are warranted to fully evaluate the potential risk of NMs across different sectors of applications.

Acknowledgements

References

ACGIH. (2021). 2021 Threshold Limit Values (TLVs) and Biological Exposure Indices (BEIs). American Conference of Governmental Industrial Hygienists. Available at: https://www.acgih.org/science/tlv-bei-guidelines/.

ANSES. (2021). Health Risk Assessment Guide for Nanomaterials in Food. French Agency for Food, Environmental and Occupational Health and Safety (ANSES). Available at: https://www.anses.fr/fr/system/files/ERCA2016SA0226.pdf. Accessed date: 01-17-2022.

Arami H, Khandhar A, Liggitt D, & Krishnan KM (2015). In vivo delivery, pharmacokinetics, biodistribution and toxicity of iron oxide nanoparticles. Chem Soc Rev, 44(23), 8576–8607. 10.1039/c5cs00541h [PubMed: 26390044]

Aureli F, Ciprotti M, D'Amato M, do Nascimento da Silva E, Nisi S, Passeri D, Sorbo A, Raggi A, Rossi M, & Cubadda F (2020). Determination of total silicon and SiO2 particles using an ICP-MS based analytical platform for toxicokinetic studies of synthetic amorphous silica. Nanomaterials, 10(5), 888. 10.3390/nano10050888 [PubMed: 32384606]

Bachler G, Losert S, Umehara Y, von Goetz N, Rodriguez-Lorenzo L, Petri-Fink A, Rothen-Rutishauser B, & Hungerbuehler K (2015). Translocation of gold nanoparticles across the lung epithelial tissue barrier: Combining in vitro and in silico methods to substitute in vivo experiments. Part Fibre Toxicol, 12, 18. 10.1186/s12989-015-0090-8 [PubMed: 26116549]

Bachler G, von Goetz N, & Hungerbuhler K (2013). A physiologically based pharmacokinetic model for ionic silver and silver nanoparticles. Int J Nanomedicine, 8, 3365–3382. 10.2147/IJN.S46624 [PubMed: 24039420]

Bachler G, von Goetz N, & Hungerbuhler K (2015). Using physiologically based pharmacokinetic (PBPK) modeling for dietary risk assessment of titanium dioxide (TiO2) nanoparticles. Nanotoxicology, 9(3), 373–380. 10.3109/17435390.2014.940404 [PubMed: 25058655]

Badrigilan S, Heydarpanahi F, Choupani J, Jaymand M, Samadian H, Hoseini-Ghahfarokhi M, Webster TJ, & Tayebi L (2020). A Review on the Biodistribution, Pharmacokinetics and Toxicity of Bismuth-Based Nanomaterials. Int J Nanomedicine, 15, 7079–7096. 10.2147/IJN.S250001 [PubMed: 33061369]

Bai X, Wang J, Mu Q, & Su G (2021). In vivo Protein Corona Formation: Characterizations, Effects on Engineered Nanoparticles' Biobehaviors, and Applications. Front Bioeng Biotechnol, 9, 646708. 10.3389/fbioe.2021.646708 [PubMed: 33869157]

Bailly AL, Correard F, Popov A, Tselikov G, Chaspoul F, Appay R, Al-Kattan A, Kabashin AV, Braguer D, & Esteve MA (2019). In vivo evaluation of safety, biodistribution and pharmacokinetics of laser-synthesized gold nanoparticles. Sci Rep, 9(1), 12890. 10.1038/s41598-019-48748-3 [PubMed: 31501470]

Baker GL, Gupta A, Clark ML, Valenzuela BR, Staska LM, Harbo SJ, Pierce JT, & Dill JA (2008). Inhalation toxicity and lung toxicokinetics of C60 fullerene nanoparticles and microparticles. Toxicol Sci, 101(1), 122–131. 10.1093/toxsci/kfm243 [PubMed: 17878152]

Balasubramanian SK, Poh K-W, Ong C-N, Kreyling WG, Ong W-Y, & Liya EY (2013). The effect of primary particle size on biodistribution of inhaled gold nano-agglomerates. Biomaterials, 34(22), 5439–5452. 10.1016/j.biomaterials.2013.03.080 [PubMed: 23639527]

Blaauboer BJ, & Andersen ME (2007). The need for a new toxicity testing and risk analysis paradigm to implement REACH or any other large scale testing initiative. Archives of toxicology, 81(5), 385–387. 10.1007/s00204-006-0175-0 [PubMed: 17262219]

Bose T, Latawiec D, Mondal PP, & Mandal S (2014). Overview of nano-drugs characteristics for clinical application: the journey from the entry to the exit point. Journal of nanoparticle research, 16(8), 1–25. 10.1007/s11051-014-2527-7

Braakhuis HM, Gosens I, Krystek P, Boere JA, Cassee FR, Fokkens PH, Post JA, van Loveren H, & Park MV (2014). Particle size dependent deposition and pulmonary inflammation after short-term inhalation of silver nanoparticles. Part Fibre Toxicol, 11, 49. 10.1186/s12989-014-0049-1 [PubMed: 25227272]

BSI. (2010). Nanotechnololgies-Part 3: Guide to assessing airborne exposure in occupational settings relevant to nanomaterials (6699–3).

Cedervall T, Lynch I, Lindman S, Berggård T, Thulin E, Nilsson H, Dawson KA, & Linse S (2007). Understanding the nanoparticle–protein corona using methods to quantify exchange rates and affinities of proteins for nanoparticles. Proceedings of the National Academy of Sciences, 104(7), 2050–2055. 10.1073/pnas.0608582104

Chandran P, Riviere JE, & Monteiro-Riviere NA (2017). Surface chemistry of gold nanoparticles determines the biocorona composition impacting cellular uptake, toxicity and gene expression profiles in human endothelial cells. Nanotoxicology, 11(4), 507–519. 10.1080/17435390.2017.1314036 [PubMed: 28420299]

Chen Q (2020). A New Dose-Response Assessment Framework with Quantitatively Integrated Information of Mode of Action for Liver Carcinogenesis. PhD Dissertation. Indiana University, Bloomington, Indiana.

Cheng YH, He C, Riviere JE, Monteiro-Riviere NA, & Lin Z (2020). Meta-Analysis of Nanoparticle Delivery to Tumors Using a Physiologically Based Pharmacokinetic Modeling and Simulation Approach. ACS Nano, 14(3), 3075–3095. 10.1021/acsnano.9b08142 [PubMed: 32078303]

Cheng YH, Riviere JE, Monteiro-Riviere NA, & Lin Z (2018). Probabilistic risk assessment of gold nanoparticles after intravenous administration by integrating in vitro and in vivo toxicity with physiologically based pharmacokinetic modeling. Nanotoxicology, 12(5), 453–469. 10.1080/17435390.2018.1459922 [PubMed: 29658401]

Chinen AB, Guan CM, Ko CH, & Mirkin CA (2017). The impact of protein corona formation on the macrophage cellular uptake and biodistribution of spherical nucleic acids. Small, 13(16), 1603847. 10.1002/smll.201603847

Cho WS, Cho M, Jeong J, Choi M, Han BS, Shin HS, Hong J, Chung BH, Jeong J, & Cho MH (2010, May 15). Size-dependent tissue kinetics of PEG-coated gold nanoparticles. Toxicol Appl Pharmacol, 245(1), 116–123. 10.1016/j.taap.2010.02.013 [PubMed: 20193702]

Choi CH, Zuckerman JE, Webster P, & Davis ME (2011). Targeting kidney mesangium by nanoparticles of defined size. Proc Natl Acad Sci U S A, 108(16), 6656–6661. 10.1073/pnas.1103573108 [PubMed: 21464325]

Choi HS, Ipe BI, Misra P, Lee JH, Bawendi MG, & Frangioni JV (2009). Tissue- and organ-selective biodistribution of NIR fluorescent quantum dots. Nano Lett, 9(6), 2354–2359. 10.1021/nl900872r [PubMed: 19422261]

Choi HS, Liu W, Misra P, Tanaka E, Zimmer JP, Itty Ipe B, Bawendi MG, & Frangioni JV (2007). Renal clearance of quantum dots. Nat Biotechnol, 25(10), 1165–1170. 10.1038/nbt1340 [PubMed: 17891134]

Choi K, Riviere JE, & Monteiro-Riviere NA (2017). Protein corona modulation of hepatocyte uptake and molecular mechanisms of gold nanoparticle toxicity. Nanotoxicology, 11(1), 64–75. 10.1080/17435390.2016.1264638 [PubMed: 27885867]

Choi SJ, & Choy JH (2014). Biokinetics of zinc oxide nanoparticles: toxicokinetics, biological fates, and protein interaction. Int J Nanomedicine, 9 Suppl 2, 261–269. 10.2147/IJN.S57920 [PubMed: 25565844]

Chou WC, Cheng YH, Riviere JE, Monteiro-Riviere NA, Kreyling WG, & Lin Z (2022). Superiority of a new route-specific versus traditional route-to-route extrapolation approach in developing a physiologically based pharmacokinetic model for gold nanoparticles in rats. The 61st Annual Meeting of Society of Toxicology, San Diego, CA. The Toxicologist, Supplement to Toxicological Sciences,186, (S1), p. 224, abstract/poster board #: 3686/P335. (March 27–31, 2022).

Chou WC, & Lin Z (2021). Development of a Gestational and Lactational Physiologically Based Pharmacokinetic (PBPK) Model for Perfluorooctane Sulfonate (PFOS) in Rats and Humans and Its Implications in the Derivation of Health-Based Toxicity Values. Environ Health Perspect, 129(3), 37004. 10.1289/EHP7671 [PubMed: 33730865]

Crump KS (1984). A new method for determining allowable daily intakes. Fundam Appl Toxicol, 4(5), 854–871. 10.1016/0272-0590(84)90107-6 [PubMed: 6510615]

Dai Q, Walkey C, & Chan WC (2014). Polyethylene glycol backfilling mitigates the negative impact of the protein corona on nanoparticle cell targeting. Angew Chem Int Ed Engl, 53(20), 5093–5096. 10.1002/anie.201309464 [PubMed: 24700480]

De Jong WH, De Rijk E, Bonetto A, Wohlleben W, Stone V, Brunelli A, Badetti E, Marcomini A, Gosens I, & Cassee FR (2019). Toxicity of copper oxide and basic copper carbonate nanoparticles after short-term oral exposure in rats. Nanotoxicology, 13(1), 50–72. 10.1080/17435390.2018.1530390 [PubMed: 30451559]

Docter D, Westmeier D, Markiewicz M, Stolte S, Knauer SK, & Stauber RH (2015). The nanoparticle biomolecule corona: lessons learned - challenge accepted? Chem Soc Rev, 44(17), 6094–6121. 10.1039/c5cs00217f [PubMed: 26065524]

Dourson M, Ewart L, Fitzpatrick SC, Barros SBM, Mahadevan B, & Hayes AW (2022). The Future of Uncertainty Factors With In Vitro Studies Using Human Cells. Toxicol Sci, 186(1), 12–17. 10.1093/toxsci/kfab134 [PubMed: 34755872]

Dourson ML, Felter SP, & Robinson D (1996). Evolution of science-based uncertainty factors in noncancer risk assessment. Regul Toxicol Pharmacol, 24(2 Pt 1), 108–120. 10.1006/rtph.1996.0116 [PubMed: 8933624]

Duan Y, Liu J, Ma L, Li N, Liu H, Wang J, Zheng L, Liu C, Wang X, Zhao X, Yan J, Wang S, Wang H, Zhang X, & Hong F (2010). Toxicological characteristics of nanoparticulate anatase titanium dioxide in mice. Biomaterials, 31(5), 894–899. 10.1016/j.biomaterials.2009.10.003 [PubMed: 19857890]

Dubaj T, Kozics K, Sramkova M, Manova A, Bastus NG, Moriones OH, Kohl Y, Dusinska M, Runden-Pran E, Puntes V, Nelson A, Gabelova A, & Simon P (2022, Feb 1). Pharmacokinetics of PEGylated Gold Nanoparticles: In Vitro-In Vivo Correlation. Nanomaterials (Basel), 12(3). 10.3390/nano12030511

EFSA. (2011). Use of BMDS and PROAST software packages by EFSA Scientific Panels and Units for applying the Benchmark Dose (BMD) approach in risk assessment. Technical Report from European Food Safety Authority, Parma, Italy. Available at: https://efsa.onlinelibrary.wiley.com/doi/epdf/10.2903/sp.efsa.2011.EN-113.

EFSA. (2021). Guidance on technical requirements for regulated food and feed product applications to establish the presence of small particles including nanoparticles. EFSA J, 19(8), e06769. 10.2903/j.efsa.2021.6769 [PubMed: 34377191]

EFSA, Hardy A, Benford D, Halldorsson T, Jeger MJ, Knutsen KH, More S, Mortensen A, Naegeli H, & Noteborn H (2017). Update: use of the benchmark dose approach in risk assessment. EFSA Journal, 15(1), e04658. [PubMed: 32625254]

EPA. (2010). Quantitative Health Risk Assessment for Particulate Matter. U.S. Environmental Protection Agency (EPA). Available at: https://www3.epa.gov/ttn/naaqs/standards/pm/data/PM_RA_FINAL_June_2010.pdf. (accessed date: March 31, 2022).

EPA. (2012). Benchmark Dose Technical Guidance. U.S. Environmental Protection Agency (EPA), Washington, DC. Available at: https://www.epa.gov/sites/default/files/2015-01/documents/benchmark_dose_guidance.pdf. Last accessed date: 01-27-2022.

EPA. (2014). Framework for Human Health Risk Assessment to Inform Decision Making. U.S. Environmental Protection Agency (EPA). Available at: https://www.epa.gov/sites/default/files/2014-12/documents/hhra-framework-final-2014.pdf. (accessed date: March 31, 2022).

EPA. (2019). Administrator Wheeler Signs Memo to Reduce Animal Testing, Awards $4.25 Million to Advance Research on Alternative Methods to Animal Testing. United States Environmental Protection Agency (EPA). Available at: https://www.epa.gov/newsreleases/administrator-wheeler-signs-memo-reduce-animal-testing-awards-425-million-advance (accessed date: March 31, 2022).

EU. (2013). Consolidated text: Regulation (EC) No 1223/2009 of the European Parliament and of the Council of 30 November 2009 on cosmetic products (recast) (Text with EEA relevance)Text with EEA relevance. . Official Journal of the European Union, L 342/359 – 342/209. https://eur-lex.europa.eu/legal-content/EN/TXT/?uri=CELEX:02009R1223-20190813

Feng S, Ren Y, Li H, Tang Y, Yan J, Shen Z, Zhang H, & Chen F (2021). Cancer Cell-Membrane Biomimetic Boron Nitride Nanospheres for Targeted Cancer Therapy. Int J Nanomedicine, 16, 2123–2136. 10.2147/IJN.S266948 [PubMed: 33731994]

Fisher J, Gearhart J, & Lin Z (2020). Physiologically Based Pharmacokinetic (PBPK) Modeling - Methods and Applications in Toxicology and Risk Assessment. First Edition. Elsevier, Inc. Pages: 1–346.

Forest V, Pourchez J, Pélissier C, Audignon Durand S, Vergnon J-M, & Fontana L (2021). Relationship between occupational exposure to airborne nanoparticles, nanoparticle lung burden and lung diseases. Toxics, 9(9), 204. 10.3390/toxics9090204 [PubMed: 34564355]

Garcia-Alvarez R, Hadjidemetriou M, Sanchez-Iglesias A, Liz-Marzan LM, & Kostarelos K (2018). In vivo formation of protein corona on gold nanoparticles. The effect of their size and shape. Nanoscale, 10(3), 1256–1264. 10.1039/c7nr08322j [PubMed: 29292433]

Garcia-Alvarez R, & Vallet-Regi M (2021). Hard and Soft Protein Corona of Nanomaterials: Analysis and Relevance. Nanomaterials (Basel), 11(4). 10.3390/nano11040888

Garcia T, Lafuente D, Blanco J, Sanchez DJ, Sirvent JJ, Domingo JL, & Gomez M (2016). Oral subchronic exposure to silver nanoparticles in rats. Food Chem Toxicol, 92, 177–187. 10.1016/j.fct.2016.04.010 [PubMed: 27090107]

Gosens I, Kermanizadeh A, Jacobsen NR, Lenz AG, Bokkers B, de Jong WH, Krystek P, Tran L, Stone V, Wallin H, Stoeger T, & Cassee FR (2015). Comparative hazard identification by a single dose lung exposure of zinc oxide and silver nanomaterials in mice. PLoS One, 10(5), e0126934. 10.1371/journal.pone.0126934 [PubMed: 25966284]

Graham UM, Jacobs G, Yokel RA, Davis BH, Dozier AK, Birch ME, Tseng MT, Oberdorster G, Elder A, & DeLouise L (2017). From Dose to Response: In Vivo Nanoparticle Processing and Potential Toxicity. Adv Exp Med Biol, 947, 71–100. 10.1007/978-3-319-47754-1_4 [PubMed: 28168666]

Haber LT, Dourson ML, Allen BC, Hertzberg RC, Parker A, Vincent MJ, Maier A, & Boobis AR (2018). Benchmark dose (BMD) modeling: current practice, issues, and challenges. Crit Rev Toxicol, 48(5), 387–415. 10.1080/10408444.2018.1430121 [PubMed: 29516780]

Halamoda-Kenzaoui B, Ceridono M, Urban P, Bogni A, Ponti J, Gioria S, & Kinsner-Ovaskainen A (2017). The agglomeration state of nanoparticles can influence the mechanism of their cellular internalisation. J Nanobiotechnology, 15(1), 48. 10.1186/s12951-017-0281-6 [PubMed: 28651541]

Hauck TS, Anderson RE, Fischer HC, Newbigging S, & Chan WC (2010). In vivo quantum-dot toxicity assessment. Small, 6(1), 138–144. 10.1002/smll.200900626 [PubMed: 19743433]

Hauser M, & Nowack B (2019). Meta-Analysis of Pharmacokinetic Studies of Nanobiomaterials for the Prediction of Excretion Depending on Particle Characteristics. Front Bioeng Biotechnol, 7, 405. 10.3389/fbioe.2019.00405 [PubMed: 31921810]

He X, Zhang H, Ma Y, Bai W, Zhang Z, Lu K, Ding Y, Zhao Y, & Chai Z (2010). Lung deposition and extrapulmonary translocation of nano-ceria after intratracheal instillation. Nanotechnology, 21(28), 285103. 10.1088/0957-4484/21/28/285103 [PubMed: 20562477]

Hegde K, Brar SK, Verma M, & Surampalli RY (2016). Current understandings of toxicity, risks and regulations of engineered nanoparticles with respect to environmental microorganisms. Nanotechnology for Environmental Engineering, 1(1), 1–12. 10.1007/s41204-016-0005-4

Heo MB, Kwak M, An KS, Kim HJ, Ryu HY, Lee SM, Song KS, Kim IY, Kwon JH, & Lee TG (2020). Oral toxicity of titanium dioxide P25 at repeated dose 28-day and 90-day in rats. Part Fibre Toxicol, 17(1), 34. 10.1186/s12989-020-00350-6 [PubMed: 32680532]

Hinderliter PM, Minard KR, Orr G, Chrisler WB, Thrall BD, Pounds JG, & Teeguarden JG (2010). ISDD: A computational model of particle sedimentation, diffusion and target cell dosimetry for in vitro toxicity studies. Part Fibre Toxicol, 7(1), 36. 10.1186/1743-8977-7-36 [PubMed: 21118529]

Hirn S, Semmler-Behnke M, Schleh C, Wenk A, Lipka J, Schaffler M, Takenaka S, Moller W, Schmid G, Simon U, & Kreyling WG (2011). Particle size-dependent and surface charge-dependent biodistribution of gold nanoparticles after intravenous administration. Eur J Pharm Biopharm, 77(3), 407–416. 10.1016/j.ejpb.2010.12.029 [PubMed: 21195759]

Hoshyar N, Gray S, Han H, & Bao G (2016). The effect of nanoparticle size on in vivo pharmacokinetics and cellular interaction. Nanomedicine (Lond), 11(6), 673–692. 10.2217/nnm.16.5 [PubMed: 27003448]

HSI. (2021). Mexico becomes first country in North America to outlaw animal testing for cosmetics. Humane Society International (HSI), Mexico. Available at: https://www.hsi.org/news-media/mexico-becomes-first-country-in-north-america-to-outlaw-animal-testing-for-cosmetics/. (accessed date: March 31, 2022).

Ji JH, Jung JH, Kim SS, Yoon JU, Park JD, Choi BS, Chung YH, Kwon IH, Jeong J, Han BS, Shin JH, Sung JH, Song KS, & Yu IJ (2007). Twenty-eight-day inhalation toxicity study of silver nanoparticles in Sprague-Dawley rats. Inhal Toxicol, 19(10), 857–871. 10.1080/08958370701432108 [PubMed: 17687717]

Khodaparast Z, van Gestel CAM, Papadiamantis AG, Goncalves SF, Lynch I, & Loureiro S (2021). Toxicokinetics of silver nanoparticles in the mealworm Tenebrio molitor exposed via soil or food. Sci Total Environ, 777, 146071. 10.1016/j.scitotenv.2021.146071 [PubMed: 33684768]

Kimmel G, Ohanian E, & Vu V (1999). Framework for human health risk assessment. Human and Ecological Risk Assessment: An International Journal, 5(5), 997–1001. 10.1080/10807039991289284

Kong B, Seog JH, Graham LM, & Lee SB (2011). Experimental considerations on the cytotoxicity of nanoparticles. Nanomedicine (Lond), 6(5), 929–941. 10.2217/nnm.11.77 [PubMed: 21793681]

Krewski D, Acosta D Jr., Andersen M, Anderson H, Bailar JC 3rd, Boekelheide K, Brent R, Charnley G, Cheung VG, Green S Jr., Kelsey KT, Kerkvliet NI, Li AA, McCray L, Meyer O, Patterson RD, Pennie W, Scala RA, Solomon GM, Stephens M, Yager J, & Zeise L (2010). Toxicity testing in the 21st century: a vision and a strategy. J Toxicol Environ Health B Crit Rev, 13(2–4), 51–138. 10.1080/10937404.2010.483176 [PubMed: 20574894]

Kreyling WG, Holzwarth U, Haberl N, Kozempel J, Hirn S, Wenk A, Schleh C, Schaffler M, Lipka J, Semmler-Behnke M, & Gibson N (2017). Quantitative biokinetics of titanium dioxide nanoparticles after intravenous injection in rats: Part 1. Nanotoxicology, 11(4), 434–442. 10.1080/17435390.2017.1306892 [PubMed: 28290717]

Kreyling WG, Holzwarth U, Haberl N, Kozempel J, Wenk A, Hirn S, Schleh C, Schaffler M, Lipka J, Semmler-Behnke M, & Gibson N (2017). Quantitative biokinetics of titanium dioxide

nanoparticles after intratracheal instillation in rats: Part 3. Nanotoxicology, 11(4), 454–464. 10.1080/17435390.2017.1306894 [PubMed: 28290735]

Kreyling WG, Holzwarth U, Schleh C, Hirn S, Wenk A, Schaffler M, Haberl N, Semmler-Behnke M, & Gibson N (2019). Quantitative biokinetics over a 28 day period of freshly generated, pristine, 20 nm titanium dioxide nanoparticle aerosols in healthy adult rats after a single two-hour inhalation exposure. Part Fibre Toxicol, 16(1), 29. 10.1186/s12989-019-0303-7 [PubMed: 31288843]

Kreyling WG, Holzwarth U, Schleh C, Kozempel J, Wenk A, Haberl N, Hirn S, Schaffler M, Lipka J, Semmler-Behnke M, & Gibson N (2017). Quantitative biokinetics of titanium dioxide nanoparticles after oral application in rats: Part 2. Nanotoxicology, 11(4), 443–453. 10.1080/17435390.2017.1306893 [PubMed: 28290734]

Kuempel ED, Geraci CL, & Schulte PA (2012). Risk assessment and risk management of nanomaterials in the workplace: translating research to practice. Ann Occup Hyg, 56(5), 491–505. 10.1093/annhyg/mes040 [PubMed: 22752094]

Kumar P, Kalaiarasan G, Porter AE, Pinna A, Klosowski MM, Demokritou P, Chung KF, Pain C, Arvind DK, Arcucci R, Adcock IM, & Dilliway C (2021, Feb 20). An overview of methods of fine and ultrafine particle collection for physicochemical characterisation and toxicity assessments. Sci Total Environ, 756, 143553. 10.1016/j.scitotenv.2020.143553 [PubMed: 33239200]

Labib S, Williams A, Yauk CL, Nikota JK, Wallin H, Vogel U, & Halappanavar S (2016). Nano-risk Science: application of toxicogenomics in an adverse outcome pathway framework for risk assessment of multi-walled carbon nanotubes. Part Fibre Toxicol, 13, 15. 10.1186/s12989-016-0125-9 [PubMed: 26979667]

Lai DY (2012). Toward toxicity testing of nanomaterials in the 21st century: a paradigm for moving forward. Wiley Interdisciplinary Reviews: Nanomedicine and Nanobiotechnology, 4(1), 1–15. 10.1002/wnan.162 [PubMed: 21965171]

Lee J-A, Kim M-K, Song JH, Jo M-R, Yu J, Kim K-M, Kim Y-R, Oh J-M, & Choi S-J (2017). Biokinetics of food additive silica nanoparticles and their interactions with food components. Colloids and Surfaces B: Biointerfaces, 150, 384–392. 10.1016/j.colsurfb.2016.11.001 [PubMed: 27842933]

Lei W, Sun C, Jiang T, Gao Y, Yang Y, Zhao Q, & Wang S (2019). Polydopamine-coated mesoporous silica nanoparticles for multi-responsive drug delivery and combined chemo-photothermal therapy. Mater Sci Eng C Mater Biol Appl, 105, 110103. 10.1016/j.msec.2019.110103 [PubMed: 31546357]

Li M, Al-Jamal KT, Kostarelos K, & Reineke J (2010). Physiologically based pharmacokinetic modeling of nanoparticles. ACS Nano, 4(11), 6303–6317. 10.1021/nn1018818 [PubMed: 20945925]

Li M, Zou P, Tyner K, & Lee S (2017, Jan). Physiologically Based Pharmacokinetic (PBPK) Modeling of Pharmaceutical Nanoparticles. AAPS J, 19(1), 26–42. 10.1208/s12248-016-0010-3 [PubMed: 27834047]

Li T, Hu H, Yang C, Zhang B, & Ma L (2021). A Study on Ecotoxicological Effects of Nano-copper Oxide Particles to Portunus trituberculatus. Curr Pharm Biotechnol, 22(4), 534–540. 10.2174/1389201021666201229111251 [PubMed: 33372870]

Li Z, Li D, Zhang W, Zhang P, Kan Q, & Sun J (2019). Insight into the preformed albumin corona on *in vitro* and *in vivo* performances of albumin-selective nanoparticles. Asian journal of pharmaceutical sciences, 14(1), 52–62. 10.1016/j.ajps.2018.07.002 [PubMed: 32104438]

Libalova H, Costa PM, Olsson M, Farcal L, Ortelli S, Blosi M, Topinka J, Costa AL, & Fadeel B (2018). Toxicity of surface-modified copper oxide nanoparticles in a mouse macrophage cell line: Interplay of particles, surface coating and particle dissolution. Chemosphere, 196, 482–493. 10.1016/j.chemosphere.2017.12.182 [PubMed: 29324388]

Lin G, Ouyang Q, Hu R, Ding Z, Tian J, Yin F, Xu G, Chen Q, Wang X, & Yong KT (2015). In vivo toxicity assessment of non-cadmium quantum dots in BALB/c mice. Nanomedicine, 11(2), 341–350. 10.1016/j.nano.2014.10.002 [PubMed: 25461291]

Lin P, Chen JW, Chang LW, Wu JP, Redding L, Chang H, Yeh TK, Yang CS, Tsai MH, Wang HJ, Kuo YC, & Yang RS (2008). Computational and ultrastructural toxicology of a nanoparticle, Quantum Dot 705, in mice. Environ Sci Technol, 42(16), 6264–6270. 10.1021/es800254a [PubMed: 18767697]

Lin Z, Chou WC, Cheng YH, He C, Monteiro-Riviere NA, & Riviere JE (2022). Predicting Nanoparticle Delivery to Tumors Using Machine Learning and Artificial Intelligence Approaches. Int J Nanomedicine, 17, 1365–1379. 10.2147/IJN.S344208 [PubMed: 35360005]

Lin Z, Jaberi-Douraki M, He C, Jin S, Yang RSH, Fisher JW, & Riviere JE (2017). Performance Assessment and Translation of Physiologically Based Pharmacokinetic Models From acslX to Berkeley Madonna, MATLAB, and R Language: Oxytetracycline and Gold Nanoparticles As Case Examples. Toxicol Sci, 158(1), 23–35. 10.1093/toxsci/kfx070 [PubMed: 28402537]

Lin Z, Monteiro-Riviere NA, Kannan R, & Riviere JE (2016). A computational framework for interspecies pharmacokinetics, exposure and toxicity assessment of gold nanoparticles. Nanomedicine (Lond), 11(2), 107–119. 10.2217/nnm.15.177 [PubMed: 26653715]

Lin Z, Monteiro-Riviere NA, & Riviere JE (2015). Pharmacokinetics of metallic nanoparticles. Wiley Interdiscip Rev Nanomed Nanobiotechnol, 7(2), 189–217. 10.1002/wnan.1304 [PubMed: 25316649]

Lin Z, Monteiro-Riviere NA, & Riviere JE (2016). A physiologically based pharmacokinetic model for polyethylene glycol-coated gold nanoparticles of different sizes in adult mice. Nanotoxicology, 10(2), 162–172. 10.3109/17435390.2015.1027314 [PubMed: 25961857]

Liu J, Wang Z, Liu FD, Kane AB, & Hurt RH (2012). Chemical transformations of nanosilver in biological environments. ACS Nano, 6(11), 9887–9899. 10.1021/nn303449n [PubMed: 23046098]

Longmire M, Choyke PL, & Kobayashi H (2008, Oct). Clearance properties of nano-sized particles and molecules as imaging agents: considerations and caveats. Nanomedicine (Lond), 3(5), 703–717. 10.2217/17435889.3.5.703 [PubMed: 18817471]

Magdolenova Z, Bilanicova D, Pojana G, Fjellsbo LM, Hudecova A, Hasplova K, Marcomini A, & Dusinska M (2012). Impact of agglomeration and different dispersions of titanium dioxide nanoparticles on the human related *in vitro* cytotoxicity and genotoxicity. J Environ Monit, 14(2), 455–464. 10.1039/c2em10746e [PubMed: 22277962]

Monteiro-Riviere NA, Inman AO, & Zhang LW (2009). Limitations and relative utility of screening assays to assess engineered nanoparticle toxicity in a human cell line. Toxicol Appl Pharmacol, 234(2), 222–235. 10.1016/j.taap.2008.09.030 [PubMed: 18983864]

Monteiro-Riviere NA, Samberg ME, Oldenburg SJ, & Riviere JE (2013). Protein binding modulates the cellular uptake of silver nanoparticles into human cells: implications for in vitro to in vivo extrapolations? Toxicology letters, 220(3), 286–293. 10.1016/j.toxlet.2013.04.022 [PubMed: 23660336]

NIOSH. (2011). Current Intelligence Bulletin 63 - Occupational Exposure to Titanium Dioxide. National Institute for Occupational Safety and Health (NIOSH). Available at: https://www.cdc.gov/niosh/docs/2011-160/pdfs/2011-160.pdf.

NIOSH. (2013). Current Intelligence Bulletin 65: Occupational Exposure to Carbon Nanotubes and Nanofibers. National Institute for Occupational Safety and Health. Available at: https://www.cdc.gov/niosh/docs/2013-145/pdfs/2013-145.pdf?id=10.26616/NIOSHPUB2013145.

Noël A, Cloutier Y, Wilkinson KJ, Dion C, Hallé S, Maghni K, Tardif R, & Truchon G (2013). Generating nano-aerosols from TiO_2 (5 nm) nanoparticles showing different agglomeration states. Application to toxicological studies. Journal of occupational and environmental hygiene, 10(2), 86–96. 10.1080/15459624.2012.748340 [PubMed: 23252512]

Noël A, Maghni K, Cloutier Y, Dion C, Wilkinson KJ, Halle S, Tardif R, & Truchon G (2012). Effects of inhaled nano-TiO_2 aerosols showing two distinct agglomeration states on rat lungs. Toxicol Lett, 214(2), 109–119. 10.1016/j.toxlet.2012.08.019 [PubMed: 22944471]

NRC. (2007). Toxicity Testing in the 21st Century: A Vision and a Strategy. National Research Council, Washington, DC. The National Academies Press. Available at: https://www.nap.edu/catalog/11970/toxicity-testing-in-the-21st-century-a-vision-and-a.

NTP. (1979). Bioassay of titanium dioxide for possible carcinogenicity. National Toxicology Program. Natl Cancer Inst Carcinog Tech Rep Ser, 97, 1–123. https://www.ncbi.nlm.nih.gov/pubmed/12806394 [PubMed: 12806394]

Oberdorster G, Castranova V, Asgharian B, & Sayre P (2015). Inhalation Exposure to Carbon Nanotubes (CNT) and Carbon Nanofibers (CNF): Methodology and Dosimetry. J Toxicol

Environ Health B Crit Rev, 18(3–4), 121–212. 10.1080/10937404.2015.1051611 [PubMed: 26361791]

Oberdorster G, Oberdorster E, & Oberdorster J (2007). Concepts of nanoparticle dose metric and response metric. Environ Health Perspect, 115(6), A290. 10.1289/ehp.115-1892118

OECD. (2017). Strategies, techniques and sampling protocols for determining the concentrations of manufactured nanomaterials in air at the workplace (ENV/JM/MONO(20117)30).

Oomen AG, Steinhäuser KG, Bleeker EA, van Broekhuizen F, Sips A, Dekkers S, Wijnhoven SW, & Sayre PG (2018). Risk assessment frameworks for nanomaterials: Scope, link to regulations, applicability, and outline for future directions in view of needed increase in efficiency. NanoImpact, 9, 1–13. 10.1016/j.impact.2017.09.001

Ortega MT, Riviere JE, Choi K, & Monteiro-Riviere NA (2017). Biocorona formation on gold nanoparticles modulates human proximal tubule kidney cell uptake, cytotoxicity and gene expression. Toxicol In Vitro, 42, 150–160. 10.1016/j.tiv.2017.04.020 [PubMed: 28433809]

OSHA. (2021). US Department of Labor Occupational Safety and Health Administration (OSHA) Occupational Chemical Database. Available at: https://www.osha.gov/chemicaldata/246.

Panyala A, Chinde S, Kumari SI, Rahman MF, Mahboob M, Kumar JM, & Grover P (2019). Comparative study of toxicological assessment of yttrium oxide nano- and microparticles in Wistar rats after 28 days of repeated oral administration. Mutagenesis, 34(2), 181–201. 10.1093/mutage/gey044 [PubMed: 30753658]

Peters TM, Ramachandran G, Park JY, & Raynor PC (2016). Assessing and managing exposures to nanomaterials in the workplace. In Assessing Nanoparticle Risks to Human Health (pp. 21–44). Elsevier. 10.1016/B978-0-323-35323-6.00002-5

Pink M, Verma N, & Schmitz-Spanke S (2020). Benchmark dose analyses of toxic endpoints in lung cells provide sensitivity and toxicity ranking across metal oxide nanoparticles and give insights into the mode of action. Toxicol Lett, 331, 218–226. 10.1016/j.toxlet.2020.06.012 [PubMed: 32562635]

Poon W, Zhang X, Bekah D, Teodoro JG, & Nadeau JL (2015). Targeting B16 tumors in vivo with peptide-conjugated gold nanoparticles. Nanotechnology, 26(28), 285101. 10.1088/0957-4484/26/28/285101 [PubMed: 26111959]

Poon W, Zhang YN, Ouyang B, Kingston BR, Wu JLY, Wilhelm S, & Chan WCW (2019). Elimination Pathways of Nanoparticles. ACS Nano, 13(5), 5785–5798. 10.1021/acsnano.9b01383 [PubMed: 30990673]

Praetorius A, Tufenkji N, Goss KU, Scheringer M, von der Kammer F, & Elimelech M (2014). The road to nowhere: equilibrium partition coefficients for nanoparticles Environmental Science: Nano, 1(4), 317–323. 10.1039/C4EN00043A

Pujalte I, Dieme D, Haddad S, Serventi AM, & Bouchard M (2017). Toxicokinetics of titanium dioxide (TiO$_2$) nanoparticles after inhalation in rats. Toxicol Lett, 265, 77–85. 10.1016/j.toxlet.2016.11.014 [PubMed: 27884615]

Qu J, Wang J, Zhang H, Wu J, Ma X, Wang S, Zang Y, Huang Y, Ma Y, Cao Y, Wu D, & Zhang T (2021). Toxicokinetics and systematic responses of differently sized indium tin oxide (ITO) particles in mice via oropharyngeal aspiration exposure. Environ Pollut, 290, 117993. 10.1016/j.envpol.2021.117993 [PubMed: 34428702]

Ramachandran G (2016). Assessing Nanoparticle Risks to Human Health (Second Edition ed.). Elsevier Inc.

Richard AM, Huang R, Waidyanatha S, Shinn P, Collins BJ, Thillainadarajah I, Grulke CM, Williams AJ, Lougee RR, Judson RS, Houck KA, Shobair M, Yang C, Rathman JF, Yasgar A, Fitzpatrick SC, Simeonov A, Thomas RS, Crofton KM, Paules RS, Bucher JR, Austin CP, Kavlock RJ, & Tice RR (2021). The Tox21 10K Compound Library: Collaborative Chemistry Advancing Toxicology. Chem Res Toxicol, 34(2), 189–216. 10.1021/acs.chemrestox.0c00264 [PubMed: 33140634]

Riviere JE (2009). Pharmacokinetics of nanomaterials: an overview of carbon nanotubes, fullerenes and quantum dots. Wiley Interdiscip Rev Nanomed Nanobiotechnol, 1(1), 26–34. 10.1002/wnan.24 [PubMed: 20049776]

Riviere JE, Jaberi-Douraki M, Lillich J, Azizi T, Joo H, Choi K, Thakkar R, & Monteiro-Riviere NA (2018). Modeling gold nanoparticle biodistribution after arterial infusion into perfused tissue: Effects of surface coating, size and protein corona. Nanotoxicology, 12(10), 1093–1112. [PubMed: 29856247]

Riviere JE, Scoglio C, Sahneh FD, & Monteiro-Riviere NA (2013). Computational approaches and metrics required for formulating biologically realistic nanomaterial pharmacokinetic models. Computational Science & Discovery, 6, 014005.

Rocha TL, Gomes T, Pinheiro JP, Sousa VS, Nunes LM, Teixeira MR, & Bebianno MJ (2015). Toxicokinetics and tissue distribution of cadmium-based Quantum Dots in the marine mussel Mytilus galloprovincialis. Environ Pollut, 204, 207–214. 10.1016/j.envpol.2015.05.008 [PubMed: 25982546]

Roy A, Zhao Y, Yang Y, Szeitz A, Klassen T, & Li SD (2017). Selective targeting and therapy of metastatic and multidrug resistant tumors using a long circulating podophyllotoxin nanoparticle. Biomaterials, 137, 11–22. 10.1016/j.biomaterials.2017.05.019 [PubMed: 28528299]

Sahneh FD, Scoglio CM, Monteiro-Riviere NA, & Riviere JE (2015). Predicting the impact of biocorona formation kinetics on interspecies extrapolations of nanoparticle biodistribution modeling. Nanomedicine (Lond), 10(1), 25–33. 10.2217/nnm.14.60 [PubMed: 25032980]

Sakulkhu U, Maurizi L, Mahmoudi M, Motazacker M, Vries M, Gramoun A, Ollivier Beuzelin MG, Vallee JP, Rezaee F, & Hofmann H (2014). Ex situ evaluation of the composition of protein corona of intravenously injected superparamagnetic nanoparticles in rats. Nanoscale, 6(19), 11439–11450. 10.1039/c4nr02793k [PubMed: 25154771]

Savage DT, Hilt JZ, & Dziubla TD (2019). In Vitro Methods for Assessing Nanoparticle Toxicity. Methods Mol Biol, 1894, 1–29. 10.1007/978-1-4939-8916-4_1 [PubMed: 30547452]

Sayers BC, Walker NJ, Roycroft JH, Germolec DR, Baker GL, Clark ML, Hayden BK, DeFord H, Dill JA, Gupta A, & Stout MD (2016). Lung deposition and clearance of microparticle and nanoparticle C60 fullerene aggregates in B6C3F1 mice and Wistar Han rats following nose-only inhalation for 13 weeks. Toxicology, 339, 87–96. 10.1016/j.tox.2015.11.003 [PubMed: 26612504]

SCCS. (2020). SCCS OPINION on Titanium dioxide (TiO_2) used in cosmetic products that lead to exposure by inhalation-SCCS/1617/20, Final Opinion Scientific Committee on Consumer Safety (SCCS). Available at: https://ec.europa.eu/health/sites/default/files/scientific_committees/consumer_safety/docs/sccs_o_238.pdf.

Schäffler M, Sousa F, Wenk A, Sitia L, Hirn S, Schleh C, Haberl N, Violatto M, Canovi M, & Andreozzi P (2014). Blood protein coating of gold nanoparticles as potential tool for organ targeting. Biomaterials, 35(10), 3455–3466. 10.1016/j.biomaterials.2013.12.100 [PubMed: 24461938]

Schleh C, Semmler-Behnke M, Lipka J, Wenk A, Hirn S, Schaffler M, Schmid G, Simon U, & Kreyling WG (2012). Size and surface charge of gold nanoparticles determine absorption across intestinal barriers and accumulation in secondary target organs after oral administration. Nanotoxicology, 6(1), 36–46. 10.3109/17435390.2011.552811 [PubMed: 21309618]

Schmid O, & Stoeger T (2016). Surface area is the biologically most effective dose metric for acute nanoparticle toxicity in the lung. Journal of Aerosol Science, 99, 133–143.

Schraufnagel DE (2020). The health effects of ultrafine particles. Exp Mol Med, 52(3), 311–317. 10.1038/s12276-020-0403-3 [PubMed: 32203102]

Shannahan J (2017). The biocorona: a challenge for the biomedical application of nanoparticles. Nanotechnol Rev, 6(4), 345–353. 10.1515/ntrev-2016-0098 [PubMed: 29607287]

Shao K, Chen Q, & Wang Z (2019). Quantifying association between liver tumor incidence and early-stage liver weight increase - An NTP data analysis. Toxicol Rep, 6, 674–682. 10.1016/j.toxrep.2019.07.001 [PubMed: 31360640]

Shi H, Magaye R, Castranova V, & Zhao J (2013). Titanium dioxide nanoparticles: a review of current toxicological data. Part Fibre Toxicol, 10, 15. 10.1186/1743-8977-10-15 [PubMed: 23587290]

Shinohara N, Oshima Y, Kobayashi T, Imatanaka N, Nakai M, Ichinose T, Sasaki T, Zhang G, Fukui H, & Gamo M (2014). Dose-dependent clearance kinetics of intratracheally administered titanium

dioxide nanoparticles in rat lung. Toxicology, 325, 1–11. 10.1016/j.tox.2014.08.003 [PubMed: 25128818]

Spruill WJ, Wade WE, DiPiro JT, Blouin RA, & Pruemer JM (2014). Chapter 7: Biopharmaceutics: Absorption. In Concepts in Clinical Pharmacokinetics, Sixth Edition. American Society of Health-System Pharmacists, Bethesda, Maryland. Pages 99–114.

Stone V, Hankin S, Aitken R, Aschberger K, Baun A, Christensen FM, Fernandes TF, Hansen SF, Hartmann NB, Hutchison GR, Johnson H, Micheletti C, Read S, Ross B, Sokull-Klueттgen B, Stark D, & Tran L (2009). ENRHES – Engineered nanoparticles: review of health and environmental safety.

Sung JH, Ji JH, Yoon JU, Kim DS, Song MY, Jeong J, Han BS, Han JH, Chung YH, Kim J, Kim TS, Chang HK, Lee EJ, Lee JH, & Yu IJ (2008). Lung function changes in Sprague-Dawley rats after prolonged inhalation exposure to silver nanoparticles. Inhal Toxicol, 20(6), 567–574. 10.1080/08958370701874671 [PubMed: 18444009]

Takenaka S, Karg E, Roth C, Schulz H, Ziesenis A, Heinzmann U, Schramel P, & Heyder J (2001). Pulmonary and systemic distribution of inhaled ultrafine silver particles in rats. Environ Health Perspect, 109 Suppl 4, 547–551. 10.1289/ehp.01109s4547

Takeuchi T, Kitayama Y, Sasao R, Yamada T, Toh K, Matsumoto Y, & Kataoka K (2017). Molecularly Imprinted Nanogels Acquire Stealth In Situ by Cloaking Themselves with Native Dysopsonic Proteins. Angew Chem Int Ed Engl, 56(25), 7088–7092. 10.1002/anie.201700647 [PubMed: 28455941]

Taleb M, Ding Y, Wang B, Yang N, Han X, Du C, Qi Y, Zhang Y, Sabet ZF, Alanagh HR, Mujeeb A, Khajeh K, & Nie G (2019). Dopamine Delivery via pH-Sensitive Nanoparticles for Tumor Blood Vessel Normalization and an Improved Effect of Cancer Chemotherapeutic Drugs. Adv Healthc Mater, 8(18), e1900283. 10.1002/adhm.201900283 [PubMed: 31379139]

Tamaru M, Akita H, Nakatani T, Kajimoto K, Sato Y, Hatakeyama H, & Harashima H (2014). Application of apolipoprotein E-modified liposomal nanoparticles as a carrier for delivering DNA and nucleic acid in the brain. International journal of nanomedicine, 9, 4267. 10.2147/IJN.S65402 [PubMed: 25228805]

Tassinari R, Cubadda F, Moracci G, Aureli F, D'Amato M, Valeri M, De Berardis B, Raggi A, Mantovani A, Passeri D, Rossi M, & Maranghi F (2014). Oral, short-term exposure to titanium dioxide nanoparticles in Sprague-Dawley rat: focus on reproductive and endocrine systems and spleen. Nanotoxicology, 8(6), 654–662. 10.3109/17435390.2013.822114 [PubMed: 23834344]

Teeguarden JG, Hinderliter PM, Orr G, Thrall BD, & Pounds JG (2007). Particokinetics in vitro: dosimetry considerations for in vitro nanoparticle toxicity assessments. Toxicol Sci, 95(2), 300–312. 10.1093/toxsci/kfl165 [PubMed: 17098817]

Tesarova B, Dostalova S, Smidova V, Goliasova Z, Skubalova Z, Michalkova H, Hynek D, Michalek P, Polanska H, & Vaculovicova M (2020). Surface-PASylation of ferritin to form stealth nanovehicles enhances in vivo therapeutic performance of encapsulated ellipticine. Applied Materials Today, 18, 100501. 10.1016/j.apmt.2019.100501

Thomas DG, Smith JN, Thrall BD, Baer DR, Jolley H, Munusamy P, Kodali V, Demokritou P, Cohen J, & Teeguarden JG (2018). ISD3: a particokinetic model for predicting the combined effects of particle sedimentation, diffusion and dissolution on cellular dosimetry for in vitro systems. Part Fibre Toxicol, 15(1), 6. 10.1186/s12989-018-0243-7 [PubMed: 29368623]

Ude VC, Brown DM, Viale L, Kanase N, Stone V, & Johnston HJ (2017). Impact of copper oxide nanomaterials on differentiated and undifferentiated Caco-2 intestinal epithelial cells; assessment of cytotoxicity, barrier integrity, cytokine production and nanomaterial penetration. Part Fibre Toxicol, 14(1), 31. 10.1186/s12989-017-0211-7 [PubMed: 28835236]

Utembe W, Clewell H, Sanabria N, Doganis P, & Gulumian M (2020). Current Approaches and Techniques in Physiologically Based Pharmacokinetic (PBPK) Modelling of Nanomaterials. Nanomaterials (Basel), 10(7). 10.3390/nano10071267

Valic MS, Halim M, Schimmer P, & Zheng G (2020). Guidelines for the experimental design of pharmacokinetic studies with nanomaterials in preclinical animal models. J Control Release, 323, 83–101. 10.1016/j.jconrel.2020.04.002 [PubMed: 32278829]

Van Broekhuizen P, Van Veelen W, Streekstra WH, Schulte P, & Reijnders L (2012). Exposure limits for nanoparticles: report of an international workshop on nano reference values. Ann Occup Hyg, 56(5), 515–524. 10.1093/annhyg/mes043 [PubMed: 22752096]

Vandebriel RJ, Tonk EC, de la Fonteyne-Blankestijn LJ, Gremmer ER, Verharen HW, van der Ven LT, van Loveren H, & de Jong WH (2014). Immunotoxicity of silver nanoparticles in an intravenous 28-day repeated-dose toxicity study in rats. Part Fibre Toxicol, 11, 21. 10.1186/1743-8977-11-21 [PubMed: 24885556]

Vats M, Mishra SK, Baghini MS, Chauhan DS, Srivastava R, & De A (2017). Near Infrared Fluorescence Imaging in Nano-Therapeutics and Photo-Thermal Evaluation. Int J Mol Sci, 18(5). 10.3390/ijms18050924

Vlasova II, Kapralov AA, Michael ZP, Burkert SC, Shurin MR, Star A, Shvedova AA, & Kagan VE (2016). Enzymatic oxidative biodegradation of nanoparticles: Mechanisms, significance and applications. Toxicol Appl Pharmacol, 299, 58–69. 10.1016/j.taap.2016.01.002 [PubMed: 26768553]

Walkey CD, & Chan WC (2012). Understanding and controlling the interaction of nanomaterials with proteins in a physiological environment. Chem Soc Rev, 41(7), 2780–2799. 10.1039/c1cs15233e [PubMed: 22086677]

Wang Y, Chen Z, Ba T, Pu J, Chen T, Song Y, Gu Y, Qian Q, Xu Y, Xiang K, Wang H, & Jia G (2013). Susceptibility of young and adult rats to the oral toxicity of titanium dioxide nanoparticles. Small, 9(9–10), 1742–1752. 10.1002/smll.201201185 [PubMed: 22945798]

Weir A, Westerhoff P, Fabricius L, Hristovski K, & von Goetz N (2012). Titanium dioxide nanoparticles in food and personal care products. Environ Sci Technol, 46(4), 2242–2250. 10.1021/es204168d [PubMed: 22260395]

Weldon BA, Griffith WC, Workman T, Scoville DK, Kavanagh TJ, & Faustman EM (2018). In vitro to in vivo benchmark dose comparisons to inform risk assessment of quantum dot nanomaterials. Wiley Interdiscip Rev Nanomed Nanobiotechnol, 10(4), e1507. 10.1002/wnan.1507 [PubMed: 29350469]

Wittmaack K (2007). In search of the most relevant parameter for quantifying lung inflammatory response to nanoparticle exposure: particle number, surface area, or what? Environ Health Perspect, 115(2), 187–194. 10.1289/ehp.9254 [PubMed: 17384763]

Włodarczyk R, & Kwarciak-Kozłowska A (2021). Nanoparticles from the cosmetics and medical industries in legal and environmental aspects. Sustainability, 13(11), 5805. 10.3390/su13115805

Xu C, Song R, Lu P, Chen J, Zhou Y, Shen G, Jiang M, & Zhang W (2020). A pH-Responsive Charge-Reversal Drug Delivery System with Tumor-Specific Drug Release and ROS Generation for Cancer Therapy. Int J Nanomedicine, 15, 65–80. 10.2147/IJN.S230237 [PubMed: 32021165]

Xu H, Li Q, Su Y, Hao Y, Yan L, & An H (2012). The Study on Toxicokinetics and Distribution of CdSe Quantum Dots in Rats. In Green Communications and Networks (pp. 1361–1365). Springer.

Xu H, Zhou J, Tang S, Kong F, Li X, Shen Z, Yan L, Chen Z, Zhao L, & Jia G (2016). Evaluation of health effect among occupational population exposed to nano-titanium dioxide: a cross-sectional study. Chinese Journal of Preventive Medicine, 50(11), 976–981. [PubMed: 27903361]

Yang L, Kuang H, Zhang W, Aguilar ZP, Xiong Y, Lai W, Xu H, & Wei H (2015). Size dependent biodistribution and toxicokinetics of iron oxide magnetic nanoparticles in mice. Nanoscale, 7(2), 625–636. 10.1039/c4nr05061d [PubMed: 25423473]

Yuan D, He H, Wu Y, Fan J, & Cao Y (2019). Physiologically Based Pharmacokinetic Modeling of Nanoparticles. J Pharm Sci, 108(1), 58–72. 10.1016/j.xphs.2018.10.037 [PubMed: 30385282]

Zang X, Zhang X, Hu H, Qiao M, Zhao X, Deng Y, & Chen D (2019). Targeted Delivery of Zoledronate to Tumor-Associated Macrophages for Cancer Immunotherapy. Mol Pharm, 16(5), 2249–2258. 10.1021/acs.molpharmaceut.9b00261 [PubMed: 30969779]

Zhang XD, Wu D, Shen X, Liu PX, Fan FY, & Fan SJ (2012). In vivo renal clearance, biodistribution, toxicity of gold nanoclusters. Biomaterials, 33(18), 4628–4638. 10.1016/j.biomaterials.2012.03.020 [PubMed: 22459191]

Zhao P, & Zhang Y (2019). The overview of methods of nanoparticle exposure assessment. In Nanotoxicity (pp. 353–367). Springer.

Zhu MT, Feng WY, Wang Y, Wang B, Wang M, Ouyang H, Zhao YL, & Chai ZF (2009). Particokinetics and extrapulmonary translocation of intratracheally instilled ferric oxide nanoparticles in rats and the potential health risk assessment. Toxicol Sci, 107(2), 342–351. 10.1093/toxsci/kfn245 [PubMed: 19023088]

Zhu Y, Gu Z, Liao Y, Li S, Xue Y, Firempong MA, Xu Y, Yu J, Smyth HD, & Xu X (2022). Improved intestinal absorption and oral bioavailability of astaxanthin using poly (ethylene glycol)-graft-chitosan nanoparticles: preparation, in vitro evaluation, and pharmacokinetics in rats. Journal of the Science of Food and Agriculture 102(3), 1002–1011. 10.1002/jsfa.11435 [PubMed: 34312873]
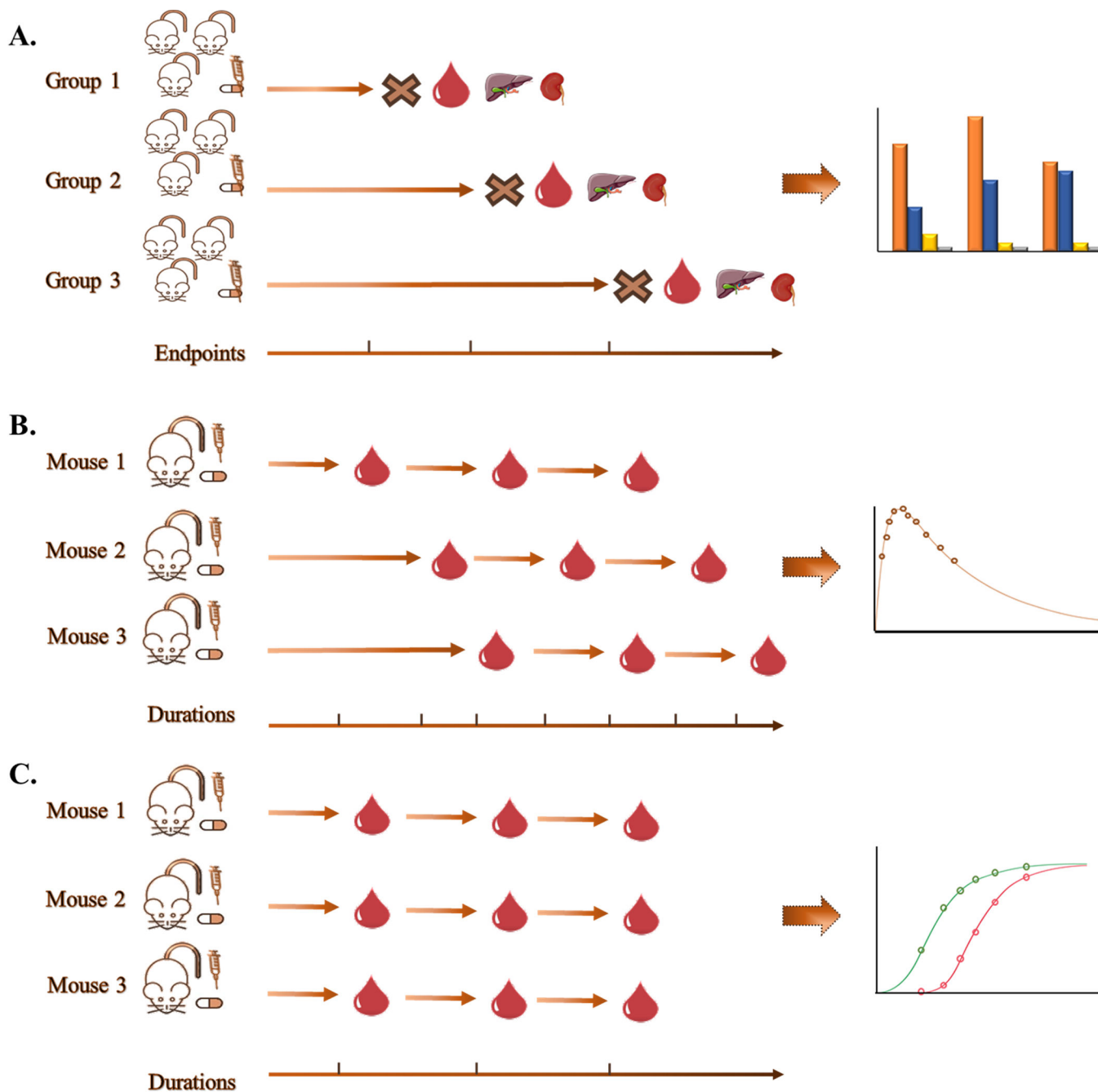
Figure 1.
The common study designs of *in vivo* studies to assess the toxicokinetics of nanoparticles. (A) The replicate sampling method in which the animals are split to multiple groups. Each group of animals are treated with a nanoparticle for a given duration or dose. At the end of the duration, the animals are sacrificed for organ and tissue collection. (B) The staggered sampling method collects the samples non-destructively at different time points and uses the subgroup data for different time points. (C) The serial sampling method collects the samples non-destructively for each individual animal at all scheduled time points. The concentration-time curves can be made for each individual animal.
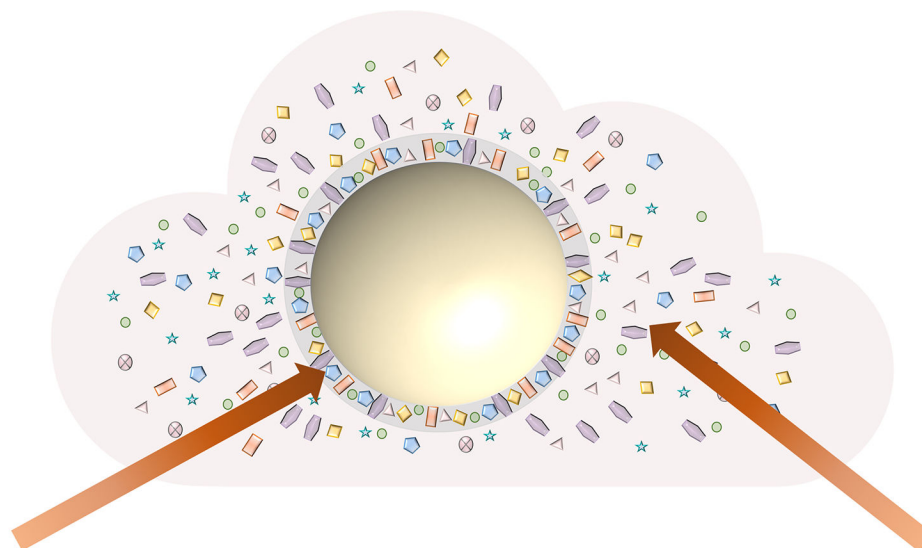
Hard Corona
- Immediately formed in seconds to minutes
- High affinity
- Strong bound proteins
- Interaction between proteins and the NM
- Low dissociation constant

Soft Corona
- Formed in hours
- Low affinity
- Weak bound proteins
- Interaction between proteins
- High dissociation constant

Figure 2.
Illustration of the hard and soft protein corona on the surface of a nanoparticle. The main differences in the characteristics between hard corona and soft corona are also listed.

Pulmonary elimination

- Aerosolic nanoparticles
- Particle size > 100 nm

RES/MPS elimination

- Particle size > 20 nm
- Uncoated NPs
- Lead to short plasma half-lives

Hepatobiliary elimination

- Particle size > 5 nm & < 100 nm

Renal elimination

- Particle size < 5 nm
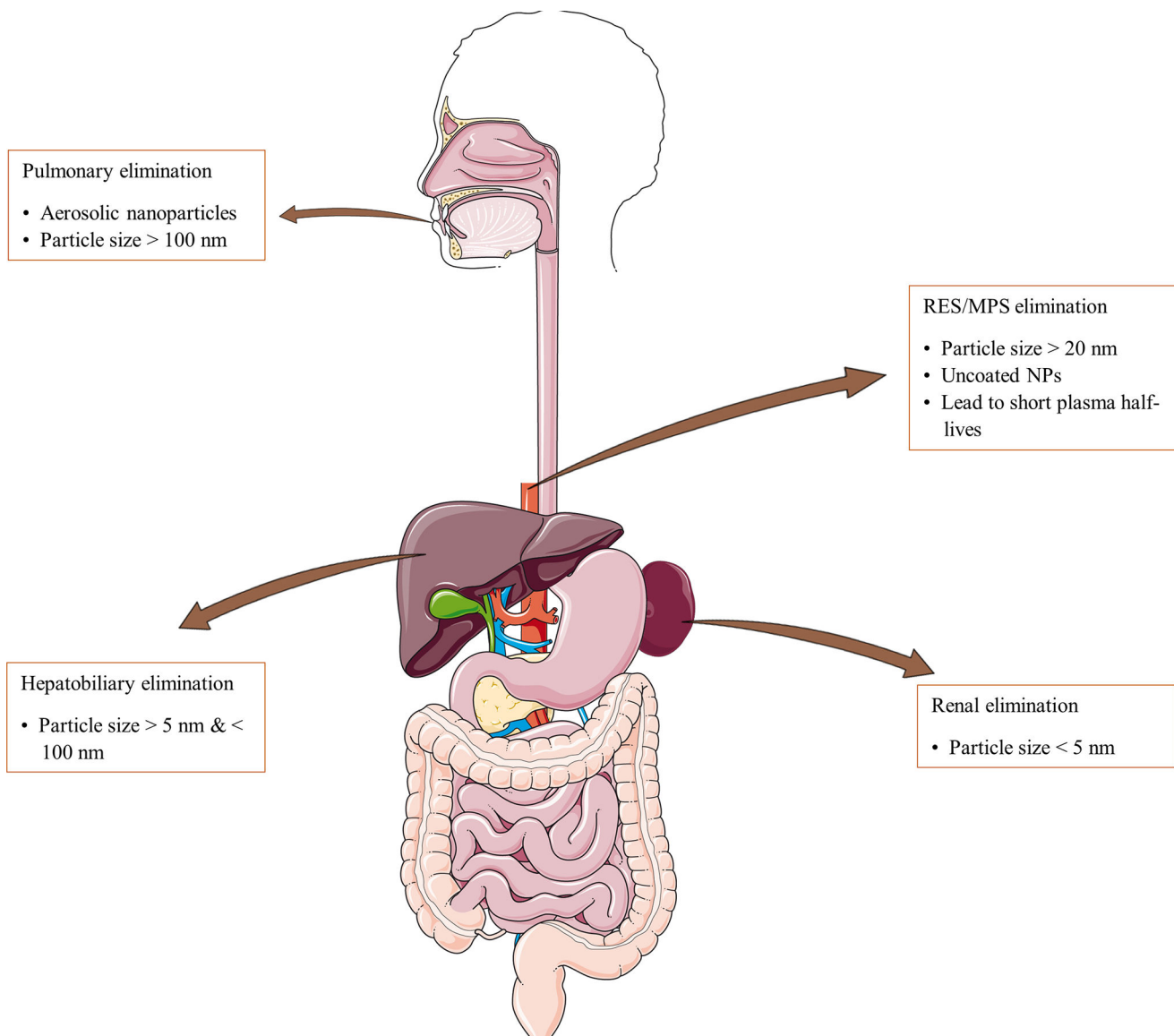
Figure 3.
The elimination routes of nanoparticles (NPs) according to their physicochemical properties.
Upon entering the body, the uncoated NPs or large NPs can be cleared by the
reticuloendothelial system (RES). Small NPs (< 5 nm) are most cleared via the renal system.
If the NP size ranges from 20 to 100 nm, the NP can be excreted through the liver. Besides,
some aerosol-based NPs with large size (> 100 nm) can be cleared via phagocytosis by
alveolar macrophages and subsequent removed through the tracheobronchial tree towards
the larynx.

Table 1.

Selected recent toxicokinetic studies of nanoparticles.

Substance	Nanoparticle Information	Model	Administration route and dosage	Study duration	Studied tissues	TK	Reference
Quantum dots	CeTe (2–7 nm)	Marine mussel	Seawater; 10 μg/L for 21 days	50 days	Whole soft tissues	Yes	(Rocha et al., 2015)
	CeSe I (2–3 nm), CeSe II (5–6 nm), CeSe III (7–8 nm), CeSe IV (2–3 nm wrapped mercaptoacetic acid)	Rats	IV, 40 mg/kg	1 min, 15 min, 45 min, 3 h, 10 h, and 24 h	Li, Ki, Te, Bl	Yes	(Xu et al., 2012)
Fullerene	55 nm and 0.93 μm	Rats	Inhalation; 2.22 mg/m^3 for 55 nm; 2.35 mg/m^3 for 0.93 μm; 3 h/day × 10 days	0, 1, 5, and 7 d	Lu	Yes	(Baker et al., 2008)
	50 nm and 1 μm	Rats, mice	Inhalation; 0.5 and 2 mg/m^3 for 50 nm; 2, 15, and 30 mg/m^3 for 1 μm; 90 days	0, 14, 28, 56 d	Lu	Yes	(Sayers et al., 2016)
Iron oxide magnetic NPs	10, 20, 30, and 40 nm	Mice	IV; 20 mg/kg	1, 3, and 7 d	Li, Lu, Sp, Ki, He, Ut, Br, St, In	No	(Yang et al., 2015)
AgNPs	uncated 50 nm AgNPs, paraffin coated 3–8 nm, PVP-stabilized 60 nm, Ag2S NPs, ionic Ag	Mealworm	Oral; 100 mg/kg 21 days	21 days	One-compartment model for the organism	Yes	(Khodaparast et al., 2021)
TiO$_2$	[^{48}V]TiO$_2$ NPs with a median agglomerate size of 70 nm	Rats	IV, oral or IT; 10 μg/rat	1 h, 4 h, 24 h, 7 d, and 28 d	Li, Lu, Sp, Ki, He, Ut, Br, Bl, Sk, Sot; Ca	Yes	(Kreyling, Holzwarth, Haberl, Kozempel, Hirn, et al., 2017; Kreyling, Holzwarth, Haberl, Kozempel, Wenk, et al., 2017; Kreyling, Holzwarth, Schleh, et al., 2017)
	20 nm (anatase)	Rats	IT; 2h		Li, Lu, Sp, Ki, He, Br, Ut, Ca, Sk, Sot, BALF, BALC	Yes	(Kreyling et al., 2019)
	20 nm	Rats	Inhalation; 6.5 mg/mL; 6h	0, 3, 6, 12, 24, 48, 72, 168, and 336 h	Li, Sp, Ki, Lu, Th, He, Ln, Br, Pa, Sg	No	(Pujalte et al., 2017)
	80% anatase +20% rutile forms, 10–100 nm	Rats	IT; 0.375, 0.75, 1.5, 3.0, and 6.0 mg/mL	1 d, 3 d, 7 d, 13 w, 26 w	Li, Lu, Ln, BALF, Tr	Yes	(Shinohara et al., 2014)
ZnO	20 and 70 nm	Rats	Oral; 50, 300, and 2000 mg/kg (single dose)	0.04, 0.25, 1, 2, 3, and 7 days	Li, Ki, Lu, Bl	Yes	(Choi & Choy, 2014)
ITO	m-ITO (120 nm) n-ITO (28 nm)	Mice	Oropharyngeal aspiration; 3.6 mg/kg and 36 mg/kg; twice/week	6 h, 18 h, 40 h, 3 d, 7 d, and 28 d	Li, Lu, Sp, Ki, He, Te	No	(Qu et al., 2021)
SiO$_2$	NM-200 (precipitated) NM-203 (thermal)	Rats	IV; 20 mg/kg (single dose or 5 days)	90 d	IV: Li, Lu, Sp, Ki, He, Br, Te	No	(Aureli et al., 2020)

Substance	Nanoparticle Information	Model	Administration route and dosage	Study duration	Studied tissues	TK	Reference
	Nano SiO$_2$ (27 nm) Bulk SiO$_2$ (4 nm)	Rats	Oral: 500 mg/kg (single dose)	6 h, 1 d, 2 d, and 3 d	Li, Lu, Sp, Ki, Bl	Yes	(Lee et al., 2017)

Abbreviations: IT: intratracheal instillation; IV: intravenous injection; TK: availability of toxicokinetic parameters; Li: liver; Lu: lung; Sp: spleen; Ki: kidney; He: heart; Th: thymus, Pa: pancreas; In: intestine; Ur: uterus; Br: brain; Bl: blood; Sk: skeleton; Sot: soft tissue; St: stomach; Ca: carcass; BALC: BAL cell; Ln: lymph node; Tr: trachea; Te: testicle; ITO: indium tin oxide; TiO$_2$: titanium dioxide; ZnO: Zinc oxide; SiO$_2$: silicon dioxide or silica.

Table 2.

Selected dose-response analysis studies of nanoparticles using the benchmark dose approach.

Reference	NP information	Experiment design	Toxicity Endpoints	Models	BMR	Software	Main findings
In vitro:							
(Pink et al., 2020)	Metal NPs, including CeO_2, CuO, TiO_2, ZnO, and ZrO_2	bronchial and alveolar epithelial cells (BEAS-2B and A549)	Oxidative stress, proliferation, mitochondrial membrane potential, enzyme activity (NQO1, CYP450, GST)	Linear, power, exponential family, polynomial family, Hill models with the lowest AIC	5%	BMDExpress	The lowest BMDs to indicate the toxicity ranking ($CeO_2 < ZrO_2 < TiO_2 < CuO < ZnO$)
(Libalova et al., 2018)	CuO with different surface modifications	mouse macrophage	cytotoxicity	Not clarified	20% relative change	PROAST	PEI-coated CuO NPs are most toxic than other coatings
(Ude et al., 2017)	CuO, $CuSO_4$	Differentiated and undifferentiated Caco2 intestinal epithelial cells	cytotoxicity	Not clarified	20% relative change	PROAST	Similar cytotoxic effects (BMD_{20}) of CuO NMs and $CuSO_4$ on undifferentiated Caco-2 cells
In vivo:							
(De Jong et al., 2019)	CuO, $Cu_2CO_3(OH)_2$	Male rats: oral gavage for 5 consecutive days	Changes in clinical chemistry and organ weights	Exponential, Hill	5% deviation	PROAST	The most sensitive endpoint of serum liver enzyme AST with BMDs of 26.2 mg/kg for CuO and 30.8 mg/kg for $Cu_2CO_3(OH)_2$
(Vandebriel et al., 2014)	Silver NPs	Male Wistar rats, repeatedly intravenous injection for 28 days	Organ weights, clinical chemistry, cytokine levels	Exponential family	5%	PROAST	The comparison the lowest bound of BMD (BMDL) showed the most sensitive endpoint of IgG level.
(Labib et al., 2016)	Multi-walled carbon nanotube	Study I: female mice, single intratracheal instillation / Study II: male mice, single pharyngeal aspiration / Study III: male mice, single pharyngeal aspiration	Transcriptional changes, lung fibrosis	Hill, Power, Linear, Polynomial	Continuous: 1.1 SD / Dichotomous: 10% excess risk	BMDExpress, BMDS	The transcriptional BMDs were consistent to that of apical results
Both in vitro and in vivo:							
(Weldon et al., 2018)	TOPO-PMAT-coated QD	*In vitro* studies; *in vivo* studies (secondary analysis)	Cytokine levels (IL6, CXCL1)	Not clarified	1 SD	BMDS	A/J strain was more sensitive to QD exposure than the C57BL/6J both *in vitro* and *in vivo* (lower BMDs)

Abbreviations: AIC, Akaike information criterion; BMD, benchmark dose; BMR, benchmark response rate; NPs, nanoparticles; SD, standard deviation; TOPO-PMAT, tri-n-octylphosphine oxide and poly(maleic anhydride-alt-1-tetradecene) co-polymer; QD, quantum dots.

Table 3.

Available exposure limits for nanomaterials.

Nanomaterials	Exposure scenarios[a]	OEL/PEL (mg/m³)	DNEL (µg/m³)	References
Organic				
Fullerene	Short-term inhalation		44.4	(Stone et al., 2009)
	Chronic inhalation		0.27	
	Short-term inhalation		201	
	Chronic inhalation		33.5	
MWCNT 10–20 nm/5–15 µm (Scenario 1: NOAEC for pulmonary effects)	Chronic inhalation (general public)		8.3	(Stone et al., 2009)
	Short-term dermal contact		7448[b]	
	Chronic dermal contact		1241[b]	
	Short-term inhalation		4	
	Chronic inhalation		0.67	
(Scenario 2: LOAEL for immune effects)	Chronic inhalation (general public)		0.17	(Stone et al., 2009)
	Short-term dermal contact		2483[b]	
	Chronic dermal contact		414[b]	
CNT	8-hour TWA	0.007		(NIOSH, 2013)
Inorganic				
AgNPs (18–19 nm)	Lung scenario 1: extrapolating factor of 3		0.33	(Stone et al., 2009)
	Lung scenario 2: extrapolating factor of 10		0.098	
	Liver effect		0.67	
TiO₂ (21 nm)	Chronic inhalation		17	(Stone et al., 2009)
TiO₂ (10–100 nm)	10 hours/day × 40 hours/week	0.3		(NIOSH, 2011)
TiO₂ (>100 nm)	10 hours/day × 40 hours/week	2.4		(NIOSH, 2011)
TiO₂ (dust)	8-hour TWA	15		(OSHA, 2021)
ZnO (Fume and respirable dust)	8-hour TWA	2		(ACGIH, 2021)
	Short-term inhalation	10		(ACGIH, 2021)
ITO	8-hour TWA	0.1		(ACGIH, 2021)

Abbreviations: CNT: carbon nanotube; DNEL: Derived no-effect level; LOAEL: lowest observed adverse effect level; MWCNT: multi-wall CNT; NOAEC: no observed adverse effect concentration; OEL: Occupational exposure limit; PEL: Permissible exposure limit; TWA: time-weighted average. Refer to Table 1 for other abbreviations.

[a]The default exposure scenarios are for workers.

[b]The unit is μg/person.